



January 2021

Modulation Of The Hyperfine Coupling In A TbPc2 Single-Molecule Magnet With Electric Fields

David Fehr

Follow this and additional works at: <https://commons.und.edu/theses>

Recommended Citation

Fehr, David, "Modulation Of The Hyperfine Coupling In A TbPc2 Single-Molecule Magnet With Electric Fields" (2021). *Theses and Dissertations*. 3924.
<https://commons.und.edu/theses/3924>

This Thesis is brought to you for free and open access by the Theses, Dissertations, and Senior Projects at UND Scholarly Commons. It has been accepted for inclusion in Theses and Dissertations by an authorized administrator of UND Scholarly Commons. For more information, please contact und.common@library.und.edu.

MODULATION OF THE HYPERFINE COUPLING IN A
TbPc₂ SINGLE-MOLECULE MAGNET WITH ELECTRIC
FIELDS

by

David Alan Fehr

B.S. in Physics, University of North Dakota, December 2019

A Thesis

Submitted to the Graduate Faculty

of the

University of North Dakota

in partial fulfillment of the requirements

for the degree of

Master of Science

Grand Forks, North Dakota


May

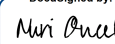
2021


Copyright 2021 David Fehr

Name: David Fehr
Degree: Master of Science

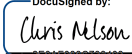
This document, submitted in partial fulfillment of the requirements for the degree from the University of North Dakota, has been read by the Faculty Advisory Committee under whom the work has been done and is hereby approved.

DocuSigned by:

76UEF80F7CCE4F...
Dr. Yen Lee Loh

DocuSigned by:

F42D61CB47C3481...
Dr. Nuri Oncel

DocuSigned by:

E44763F9A06D49B...
Dr. Deniz Cakir

This document is being submitted by the appointed advisory committee as having met all the requirements of the School of Graduate Studies at the University of North Dakota and is hereby approved.

DocuSigned by:

2E0A7088C733403...
Chris Nelson
Dean of the School of Graduate Studies

5/3/2021

Date

Permission

Title Modulation of the Hyperfine Coupling in a TbPc₂ Single-Molecule Magnet with Electric Fields

Department Physics & Astrophysics

Degree Master of Science

In presenting this thesis in partial fulfillment of the requirements for a graduate degree from the University of North Dakota, I agree that the library of this University shall make it freely available for inspection. I further agree that permission for extensive copying for scholarly purposes may be granted by the professor who supervised my thesis work or, in his absence, by the chairperson of the department or the dean of the School of Graduate Studies. It is understood that any copying or publication or other use of this thesis or part thereof for financial gain shall not be allowed without my written permission. It is also understood that due recognition shall be given to me and to the University of North Dakota in any scholarly use which may be made of any material in my thesis.

David Fehr
May 7, 2021

Acknowledgements

I would first like to thank my advisor, Dr. Loh, who has been crucial to my success at UND. His steadfast support aside, he has taught an incredible amount of things to me as my advisor and professor. During these seven years at UND I have grown tremendously as a student, and I truly believe that I owe most of this to Dr. Loh. I could not have asked for a better advisor.

Next, I would like to thank some of the professors who have been instrumental in my success at UND and have set me up for future success. I would specifically like to thank Dr. William Schwalm, Dr. Graeme Dewar, Dr. Nuri Oncel, and Dr. Deniz Çakır, whose classes built the foundation of my knowledge of physics. While I may not have fully appreciated the rigor of their classes at the time, I now recognize the value in these tribulations and I am grateful for these experiences. I would also like to thank Dr. Nuri Oncel and Dr. Deniz Çakır for agreeing to be members of my committee, their guidance, and their time in reviewing my thesis and their time in certifying my defense of it. In addition, I would like to thank Dr. Mizuho Schwalm for all of her knowledge in the realm of laboratory physics, and her support of me as a lab TA. Finally, I would like to thank Dr. Kanishka Marasinghe who has been helpful in all advising and official works. I would like to especially thank him for all advising help regarding the B.S.-M.S. program.

I would also like to thank UND and the physics department for supporting me with scholarships and assistantships. As a young, married graduate student I cannot imagine what we would have done without this financial support.

Finally, I want to thank my past cohort of undergraduate students, and my present cohort of graduate students that never fail to brighten my day. While I am ready to move on from Grand Forks, I will always cherish the time I have spent here and the wonderful people I have met.

To my parents, Kris and Alan Fehr; my sisters Laura and Karla Fehr; and my wife, Bethany Fehr, for their unwavering support and encouragement.

ABSTRACT

In theory, a quantum computer can do everything a classical computer can do, and more. This is possible because of the principal difference between their respective fundamental units of computation. Classical computers use bits that can take on values of 0 or 1, but quantum computers use quantum bits, called qubits, that can take on values of 0, 1, or any combination of 0 and 1 by exploiting the rules of quantum mechanics. However, this quantum nature is extremely fragile and therefore it is imperative that qubits are protected from their environment. Conversely, qubits cannot be so isolated that their manipulation, necessary for any basic computation, becomes impossible. One approach to realizing these qubits is by using single-molecule magnets (SMMs).

Recent experiments^{1,2} were able to achieve electrical control of a TbPc_2 SMM nuclear spin qubit via the hyperfine Stark effect (HSE). TbPc_2 consists of a terbium (III) ion sandwiched between two phthalocyanine molecules, referred to as the organic ligands. The nuclear spin qubits are well isolated from the environment, but this also makes them more difficult to manipulate since their manipulation is only achieved by using the electron spins as mediators.

The purpose of this project is two-fold and ongoing. First, we aim to understand the hyperfine Stark effect in TbPc_2 from first principles. We do this by building up a theoretical quantum mechanical framework from single-electron atoms and then generalizing the results to many-electron atoms, as shown in chapters 1 through 3. In chapter 3, we assume the ligands give rise to easy-axis anisotropy and thus we

glean an order-of-magnitude estimate of the splittings. By computing the hyperfine splittings in both the LS coupling and jj coupling schemes, we calculate a range of values which agrees with Ref. 1.

The second aim of this project is to investigate whether the HSE can be enhanced by modifying the organic ligand structures to allow for easier qubit manipulation. In chapter 4 we present a path toward this goal, starting with the procurement of TbPc_2 's electrostatic charge distribution with density functional theory. From there, we sketch out what it would take to calculate the hyperfine splittings, and how the organic ligand structures may be altered to enhance the HSE.

TABLE OF CONTENTS

| | |
|--|----------|
| ACKNOWLEDGEMENTS | v |
| ABSTRACT | vii |
| LIST OF FIGURES | 1 |
| CHAPTER: | |
| 1 Single-Electron Hydrogenic Atoms | 2 |
| 1.1 The Full One-Body Hamiltonian | 2 |
| 1.2 The Hyperfine Hamiltonian | 4 |
| 1.3 The Effective Hamiltonian due to the Coupling of the Electron and Nuclear Spins | 5 |
| 1.4 “Classical” Derivation of Hyperfine Couplings | 6 |
| 1.5 “Quantum” Derivation of Hyperfine Couplings | 8 |
| 1.6 Quantum Hyperfine Couplings in the Classical Limit | 12 |
| 1.7 The Effective Hamiltonian due to the Coupling of the Electron Angu- lar Momentum and the Nuclear Spin | 13 |
| 1.8 The Hyperfine Splitting in Hydrogen 1s | 15 |
| 1.9 The Hyperfine Stark Effect in Hydrogen 1s | 17 |
| 1.10 The Degenerate Hyperfine Stark Effect in Hydrogen $ 2lm\rangle$ | 24 |
| 1.11 Combining \hat{H}_{SI} and \hat{H}_{LI} to obtain $\hat{H}_{JI}^{\text{eff}}$ | 28 |

| | | |
|----------|--|-----------|
| 2 | Multi-Electron Atoms | 31 |
| 2.1 | The Full Many-Body Hamiltonian | 31 |
| 2.2 | Hund's Rules | 32 |
| 2.3 | Many-Body Eigenstates and Hyperfine Inner Products | 33 |
| 2.4 | Many-Body Spin Operators | 35 |
| 3 | Triply Ionized Terbium | 37 |
| 3.1 | Electronic Configuration and Ground State | 37 |
| 3.2 | The Effective 6-Particle State | 38 |
| 3.3 | LS vs. jj Coupling | 39 |
| 3.4 | Hyperfine Splittings in the LS Coupling Scheme | 40 |
| 3.5 | Hyperfine Splittings in the jj Coupling Scheme | 42 |
| 3.6 | The Hyperfine Stark Effect | 44 |
| 4 | The Hyperfine Stark Effect in TbPc₂ | 46 |
| 4.1 | Introduction to Density Functional Theory | 46 |
| 4.2 | TbPc ₂ | 47 |
| 4.3 | VASP Calculations | 47 |
| 5 | Conclusions and Future Work | 50 |
| 5.1 | Conclusions | 50 |
| 5.2 | Future Work | 51 |
| | APPENDICES | 54 |
| A1 | Wigner 3-j Symbols | 54 |
| A1.1 | Symmetry Properties | 54 |
| A1.2 | Selection rules | 54 |
| A1.3 | Relation to Clebsch-Gordan Coefficients | 55 |

| | | |
|-------------------|---|-----------|
| A1.4 | Relation to Spherical Harmonics | 55 |
| A2 | Gaunt Coefficients | 55 |
| A2.1 | Relation to Spherical Harmonic and Wigner 3-j symbols . . . | 55 |
| REFERENCES | | 55 |

List of Figures

| | | |
|-----|--|----|
| 1.1 | Hyperfine splitting diagram of Hydrogen 1s | 16 |
| 1.2 | Hyperfine Stark effect splitting diagram of Hydrogen 1s | 24 |
| 1.3 | Hyperfine Stark effect splitting diagram of Hydrogen 2s | 28 |
| 3.1 | Approximate energy level diagram of the $ J = 6, M_J\rangle$ states of Tb^{3+} due to the phthalocyanine ligands | 42 |
| 4.1 | Structural diagram of one phthalocyanine ligand. | 47 |
| 4.2 | Rendering of TbPc_2 in VESTA | 48 |
| 4.3 | Rendering of the CHGCAR file in VESTA | 49 |

CHAPTER 1

SINGLE-ELECTRON HYDROGENIC ATOMS

1.1 The Full One-Body Hamiltonian

The total energy of a hydrogenic atom is mainly due to the bare Hamiltonian, containing kinetic energy and Coulomb potential energy terms:

$$\hat{H}_0 = \frac{\hat{p}^2}{2m_e} - \frac{e^2 Z_{\text{eff}}}{4\pi\epsilon_0 r}, \quad (1.1)$$

where Z_{eff} is an effective nuclear charge ($Z_{\text{eff}} = 1$ for hydrogen). The eigenstates and energies of \hat{H}_0 are well-known³:

$$\hat{H}_0 \psi_{nlm}(\vec{r}) = E_n \psi_{nlm}(\vec{r})$$

where $E_n = -\frac{Z_{\text{eff}}^2 e^2}{8\pi\epsilon_0 a_0 n^2} = -\frac{Z_{\text{eff}}^2}{n^2} \times 13.6 \text{ eV}$ (-13.6 eV for the ground state of Hydrogen) and ψ_{nlm} is defined in terms of the well-known radial wavefunctions and spherical harmonics: $\psi_{nlm}(\vec{r}) = R_{nl}(r)Y_l^m(\theta, \phi)$. While \hat{H}_0 describes the majority of the energy, there are other, albeit smaller, contributions to the energy known as the fine structure.

The first fine-structure term of note is the relativistic correction to the kinetic energy. The kinetic energy term in \hat{H}_0 assumes a classical picture, but this can be corrected using the energy-momentum relation from special relativity³: $E^2 = (pc)^2 + (mc^2)^2$. Using this relativistic form of the kinetic energy, the first-order perturbation to \hat{H}_0 due to relativistic effects is given by $\hat{H}_{rel} = -\frac{\hat{p}^4}{8m_e^3 c^2}$. The first-order energy correction given by first-order perturbation theory is the expectation value of \hat{H}_{rel}

with respect to the eigenstates of \hat{H}_0 : $E_{rel}^{(1)} = -\frac{E_n^2}{2m_e c^2} \left(\frac{4n}{l+\frac{1}{2}} - 3 \right) \approx -9.056 \times 10^{-4} \text{eV}$ for the ground state of Hydrogen.

Another contribution to the fine structure is known as spin-orbit coupling. In the rest frame of the electron, assuming a classical picture, the nucleus appears to orbit the electron. This orbital motion creates a current and therefore a magnetic field which couples to the spin of the electron. However, in the quantum picture we have wavefunctions and so these particles do not orbit, truly speaking. Nonetheless, an expression can be found that relates the orbital motion of the nucleus with the orbital angular momentum operator of the electron. Thus, the spin angular momentum and orbital angular momentum of the electron couple to each other, and this interaction takes the form³ $\hat{H}_{SOC} = \frac{1}{2} \left(\frac{Ze^2}{4\pi\epsilon_0} \right) \left(\frac{|g_e|}{2m_e^2 c^2 r^3} \right) \vec{L} \cdot \vec{S}$, after including the relativistic Thomas correction factor. The first-order energy correction given by first-order perturbation theory is the expectation value of \hat{H}_{SOC} with respect to the eigenstates of \hat{H}_0 :

$$E_{SOC}^{(1)} = \frac{E_n^2}{m_e c^2} 2n \left(\frac{j(j+1) - l(l+1) - S(S+1)}{l(2l+1)(l+1)} \right) \sim 10^{-5} \text{ eV for the ground state of Hydrogen.}$$

There is also a non-relativistic contribution to the fine structure, called the Darwin term, which only affects s orbitals. If we look at the first-order spin-orbit correction energy it appears as though s orbitals experience spin-orbit coupling, which is incorrect. The Darwin term replaces this fictional effect in $E_{SOC}^{(1)}$ to make the formula correct. Physically, it can be interpreted as rapid quantum fluctuations of these electrons, which allows for the creation of virtual electron-positron pairs. The inclusion of the interaction between these virtual electron-positron pairs and the s orbitals raises the energy of the s orbitals to make them degenerate with the p orbitals once again. There is another effect, called the Lamb shift, which give the s orbitals a higher energy than the p orbitals, but that discussion is neglected here.

After taking these corrections into account, we uncover the fine structure of hydrogenic atoms given by the total first-order energy corrections:

$$E_{fine}^{(1)} = \frac{E_n(Z\alpha^2)}{n} \left(\frac{1}{j+\frac{1}{2}} - \frac{3}{4n} \right)$$

where we have introduced the dimensionless fine-structure constant, $\alpha = \frac{e^2}{4\pi\epsilon_0\hbar c} \approx \frac{1}{137}$. To obtain the exact energy correction and a more accurate fine structure one must solve the Dirac equation, but that discussion is not included here.

There is one more contribution to the energy that we have not yet discussed, the hyperfine structure, which most of this paper is devoted to. It describes the coupling of the electron spin and orbital angular momentum to the spin angular momentum of the nucleus, and is of interest in the realm of quantum information. Since we are more interested in the energy level splitting between these hyperfine states than actual energy values, and since the fine structure is large compared to the hyperfine structure, we need only use the fine structure to determine the ground state manifold of hyperfine states.

1.2 The Hyperfine Hamiltonian

The Hyperfine Hamiltonian has two main contributions, which are the coupling of the nuclear and electronic spins, and the coupling of the nuclear spin with the orbital angular momentum of the electron:

$$\hat{H}_{HF} = \hat{H}_{SI} + \hat{H}_{LI}. \tag{1.2}$$

1.3 The Effective Hamiltonian due to the Coupling of the Electron and Nuclear Spins

The energy due to the coupling of the magnetic dipole field of the nucleus with the magnetic moment of the electron is given by the following Hamiltonian:

$$\hat{H}_{SI} = -\vec{m}_e \cdot \vec{B}_I(\vec{r}). \quad (1.3)$$

The magnetic field at \vec{r} due to the magnetic dipole moment of the nucleus is given by

$$\vec{B}_I(\vec{r}) = \mu_0 \left[\frac{3(\vec{m}_N \cdot \vec{r})\vec{r} - r^2\vec{m}_N}{4\pi r^5} + \frac{2}{3}\vec{m}_N\delta(\vec{r}) \right]. \quad (1.4)$$

The magnetic dipole moment of the nucleus is proportional to the nuclear spin operator, \vec{I} , by $\vec{m}_I = \frac{g_N\mu_N}{\hbar}\vec{I}$, where g_N is the g-factor of the particular system's nucleus and μ_N is the nuclear magneton. Thus, the Magnetic Field at \vec{r} due to the spin of the nucleus is given by:

$$\vec{B}_I(\vec{r}) = \frac{\mu_0\mu_N g_N}{\hbar} \left[\frac{3(\vec{I} \cdot \vec{r})\vec{r} - r^2\vec{I}}{4\pi r^5} + \frac{2}{3}\delta(\vec{r})\vec{I} \right]. \quad (1.5)$$

The magnetic moment of the electron is proportional to the electron spin operator, \vec{S} , by $\vec{m}_e = -\frac{|g_e|\mu_B}{\hbar}\vec{S}$, where g_e is the g-factor of the electron and μ_B is the Bohr magneton. Thus, \hat{H}_{SI} can be written in terms of \vec{S} and \vec{I} :

$$\hat{H}_{SI} = \frac{\mu_0\mu_N\mu_B g_N |g_e|}{\hbar^2} \left[\frac{3(\vec{I} \cdot \vec{r})(\vec{S} \cdot \vec{r}) - r^2(\vec{S} \cdot \vec{I})}{4\pi r^5} + \frac{2}{3}\delta(\vec{r})(\vec{S} \cdot \vec{I}) \right]. \quad (1.6)$$

However, since the hyperfine energy splittings are several orders of magnitude smaller than the energy splittings of the bare Hamiltonian and fine structure, \hat{H}_{HF} can be treated as a perturbation. Therefore, first-order hyperfine energy splittings due to the coupling of the electron and nuclear spins will be given by

$$\begin{aligned}
E_{SI} &= \langle \psi | \hat{H}_{SI} | \psi \rangle \\
&= \frac{\mu_0 \mu_N \mu_B g_N |g_e|}{\hbar^2} \int \psi^*(\vec{r}) \left[\frac{3(\vec{I} \cdot \vec{r})(\vec{S} \cdot \vec{r}) - r^2(\vec{S} \cdot \vec{I})}{4\pi r^5} + \frac{2}{3}(\vec{S} \cdot \vec{I})\delta(\vec{r}) \right] \psi(\vec{r}) d^3r.
\end{aligned} \tag{1.7}$$

1.4 “Classical” Derivation of Hyperfine Couplings

We begin by treating \vec{S} and \vec{I} as classical vectors that point along the z-axis: $\vec{S} \equiv \hat{S}_z \hat{e}_z$ and $\vec{I} \equiv \hat{I}_z \hat{e}_z$. To obtain an expression for E_{SI} in terms of S_z , I_z , and the hyperfine couplings, we first integrate out position degrees of freedom. We do this by taking the inner product with respect to the spatial states and leaving the spin states to be determined later. Here we assume $|\psi\rangle$ is an eigenstate of the bare hydrogenic Hamiltonian, $|\psi\rangle \equiv |\psi_{nlm}\rangle$ and $\psi_{nlm}(\vec{r}) \equiv \langle \vec{r} | \psi_{nlm} \rangle = R_{nl}(r)Y_l^m(\theta, \phi)$, but later we will see that superposition states are not difficult to deal with. After implementing these assumptions, E_{SI} simplifies in the following way:

$$\begin{aligned}
E_{SI} &= \frac{\mu_0 \mu_N \mu_B g_N |g_e|}{\hbar^2} \int \psi_{nlm}(\vec{r})^* \left[\frac{3I_z S_z z^2 - r^2 I_z S_z}{4\pi r^5} + \frac{2}{3} I_z S_z \delta(\vec{r}) \right] \psi_{nlm}(\vec{r}) d^3r \\
&= \frac{\mu_0 \mu_N \mu_B g_N |g_e| S_z I_z}{\hbar^2} \int |\psi_{nlm}(\vec{r})|^2 \left[\frac{3 \cos^2 \theta - 1}{4\pi r^3} + \frac{2}{3} \delta(\vec{r}) \right] d^3r \\
&= \frac{\mu_0 \mu_N \mu_B g_N |g_e| S_z I_z}{\hbar^2} \left[\int |\psi_{nlm}(\vec{r})|^2 \frac{3 \cos^2 \theta - 1}{4\pi r^3} d^3r + \frac{2}{3} |\psi_{nlm}(\vec{0})|^2 \right].
\end{aligned} \tag{1.8}$$

The Dirac delta function is often referred to as the “contact term,” as it only contributes when the electron’s wave function is finite at the nucleus. In the last step,

we have taken advantage of the properties of the Dirac delta function. If $l = 0$ we have the spherically symmetric s orbitals, the only orbitals that are finite at the origin. Furthermore, in the $l = 0$ limit, we notice that the remaining angular integral is essentially an integral over two spherical harmonics, Y_2^0 and Y_0^0 , times a constant, Y_0^0 , and so the integral vanishes due to orthogonality. Thus, for $l = 0$, E_{SI} greatly simplifies:

$$\begin{aligned} E_{SI} &= \frac{\mu_0 \mu_N \mu_B g_N |g_e| S_z I_z}{\hbar^2} \frac{2}{3} |\psi_{n00}(\vec{0})|^2 \\ &= \frac{2\mu_0 \mu_N \mu_B g_N |g_e| S_z I_z}{3\hbar^2} \frac{Z_{\text{eff}}^3}{\pi n^3 a_0^3} = \frac{2}{3} \frac{E_0(n)}{\hbar^2} S_z I_z \equiv \frac{\alpha_{n00}^c}{\hbar^2} S_z I_z \end{aligned} \quad (1.9)$$

where we have defined $E_0(n) \equiv \frac{Z_{\text{eff}}^3 \mu_0 \mu_N \mu_B g_N |g_e|}{\pi n^3 a_0^3}$, which is an energy scale for hyperfine splittings in the shell of the atom being considered. For hydrogen ($n = 1$, $Z_{\text{eff}} = 1$, $g_N \equiv g_p$) $E_0 = 1.58 \mu\text{eV}$. We have also introduced the hyperfine structure constant for the s orbitals in the classical limit, α_{n00}^c , which has units of energy.

In the $l > 0$ limit, the contact term vanishes due to these orbitals vanishing at the origin. In these cases, only the first term remains:

$$\begin{aligned} E_{SI} &= \frac{\mu_0 \mu_N \mu_B g_N |g_e| S_z I_z}{\hbar^2} \int |\psi_{nlm}(\vec{r})|^2 \frac{3 \cos^2 \theta - 1}{4\pi r^3} d^3 r \\ &= \frac{\mu_0 \mu_N \mu_B g_N |g_e| S_z I_z}{\hbar^2} \int_0^\infty \frac{|R_{nl}|^2}{4\pi r^3} r^2 dr \int_0^\pi \int_0^{2\pi} \sin \theta |Y_l^m|^2 (3 \cos^2 \theta - 1) d\theta d\phi \\ &= \frac{\mu_0 \mu_N \mu_B g_N |g_e| S_z I_z}{\hbar^2} \left\langle \frac{1}{4\pi r^3} \right\rangle \int_0^\pi \int_0^{2\pi} \sin \theta |Y_l^m|^2 (3 \cos^2 \theta - 1) d\theta d\phi. \end{aligned} \quad (1.10)$$

It turns out that the expectation $\left\langle \frac{1}{4\pi r^3} \right\rangle$ can be expressed in terms of n and l as $\left\langle \frac{1}{4\pi r^3} \right\rangle = \frac{(Z_{\text{eff}})^3}{2\pi a_0^3 l(l+1)(2l+1)n^3}$. We can also replace the angular integral with an expression in terms of l and m with Gaunt coefficients (see Appendix A2). We begin by writing

all factors in terms of spherical harmonics:

$$\begin{aligned}
\int \sin \theta |Y_l^m|^2 (3 \cos^2 \theta - 1) d\theta d\phi &= \int \sin \theta (-1)^m Y_l^{-m} Y_l^m 4 \sqrt{\frac{\pi}{5}} Y_2^0 d\theta d\phi \\
&= (-1)^m \sqrt{\frac{16\pi}{5}} \int \sin \theta Y_l^{-m} Y_l^m Y_2^0 d\theta d\phi \\
&\equiv (-1)^m \sqrt{\frac{16\pi}{5}} \text{Gaunt}(l, l, 2, -m, m, 0) \\
&\equiv 2 \frac{l(l+1) - 3m^2}{(2l+3)(2l-1)}. \tag{1.11}
\end{aligned}$$

Putting the expressions for the radial and angular integrals back together in terms of n , l , and m we obtain:

$$\begin{aligned}
E_{SI} &= \frac{\mu_0 \mu_N \mu_B g_N |g_e|}{\hbar^2} \frac{(Z_{\text{eff}})^3}{2\pi a_0^3 l(l+1)(2l+1)n^3} 2 \frac{l(l+1) - 3m^2}{(2l+3)(2l-1)} S_z I_z \\
&= \frac{l(l+1) - 3m^2}{l(l+1)(2l+1)(2l+3)(2l-1)} \frac{E_0(n)}{\hbar^2} S_z I_z \equiv \frac{\alpha_{nlm}^c}{\hbar^2} S_z I_z \tag{1.12}
\end{aligned}$$

where we have introduced the hyperfine structure constant for the p, d, f, etc. orbitals in the classical limit, α_{nlm}^c . Putting in values for l explicitly, we finally obtain:

$$l = 0 \quad E_{SI} = \frac{2}{3} \frac{E_0(n)}{\hbar^2} S_z I_z \equiv \frac{\alpha_{n00}^c}{\hbar^2} S_z I_z \tag{1.13}$$

$$l = 1 \quad E_{SI} = \frac{1}{12} \left(\frac{4 - 6m^2}{5} \right) \frac{E_0(n)}{\hbar^2} S_z I_z \equiv \frac{\alpha_{n1m}^c}{\hbar^2} S_z I_z \tag{1.14}$$

$$l = 2 \quad E_{SI} = \frac{1}{60} \left(\frac{4 - 2m^2}{7} \right) \frac{E_0(n)}{\hbar^2} S_z I_z \equiv \frac{\alpha_{n2m}^c}{\hbar^2} S_z I_z \tag{1.15}$$

$$l = 3 \quad E_{SI} = \frac{1}{168} \left(\frac{8 - 2m^2}{15} \right) \frac{E_0(n)}{\hbar^2} S_z I_z \equiv \frac{\alpha_{n3m}^c}{\hbar^2} S_z I_z \tag{1.16}$$

1.5 “Quantum” Derivation of Hyperfine Couplings

In general, \vec{S} and \vec{I} are not simply classical vectors pointing along the z-axis. Each vector has quantum mechanical spin operators as components:

$$\vec{S} \equiv \hat{S}_x \hat{e}_x + \hat{S}_y \hat{e}_y + \hat{S}_z \hat{e}_z \text{ and } \vec{I} \equiv \hat{I}_x \hat{e}_x + \hat{I}_y \hat{e}_y + \hat{I}_z \hat{e}_z$$

As with the classical case, we will obtain an expression for E_{SI} in terms of \vec{S} , \vec{I} , and the hyperfine structure constants by taking the inner product with respect to the spatial states and leaving the spin states to be determined later. Once again, we assume $|\psi\rangle$ is an eigenstate of the bare hydrogenic Hamiltonian, $|\psi\rangle \equiv |\psi_{nlm}\rangle$ and $\psi_{nlm}(\vec{r}) \equiv \langle \vec{r} | \psi_{nlm} \rangle = R_{nl}(r) Y_l^m(\theta, \phi)$. However, we will let $\langle \psi | \equiv \langle \psi_{nlm'} |$ and $\psi_{nlm'}(\vec{r})^* \equiv \langle \psi_{nlm'} | \vec{r} \rangle = R_{nl}(r) Y_l^{m'*}(\theta, \phi)$, in order to obtain an effective electron spin-nuclear spin Hamiltonian $\hat{H}_{SI}^{\text{eff}}$ such that

$$\begin{aligned} \langle m'_l | \hat{H}_{SI}^{\text{eff}} | m_l \rangle &\equiv \langle \psi_{nlm'} | \hat{H}_{SI} | \psi_{nlm} \rangle \\ &= \frac{\mu_0 \mu_N \mu_B g_N |g_e|}{\hbar^2} \int \psi_{nlm'}(\vec{r})^* \left[\frac{3(\vec{S} \cdot \vec{r})(\vec{I} \cdot \vec{r}) - r^2(\vec{S} \cdot \vec{I})}{4\pi r^5} + \frac{2}{3}(\vec{S} \cdot \vec{I})\delta(\vec{r}) \right] \psi_{nlm}(\vec{r}) d^3r \\ &= \frac{\mu_0 \mu_N \mu_B g_N |g_e|}{\hbar^2} \left[\int \psi_{nlm'}(\vec{r})^* \left(\frac{3(\vec{S} \cdot \vec{r})(\vec{I} \cdot \vec{r}) - r^2(\vec{S} \cdot \vec{I})}{4\pi r^5} \right) \psi_{nlm}(\vec{r}) d^3r + \frac{2}{3}(\vec{S} \cdot \vec{I})\psi_{nlm'}(\vec{0})\psi_{nlm}(\vec{0}) \right] \end{aligned} \quad (1.17)$$

where in the last step we have simplified the second term in the integrand by taking advantage of the Dirac delta's properties. Furthermore, only s orbitals are finite at the origin, and in this case $m = m' = 0$. Therefore, we can further simplify the second term with the help of a Kronecker delta, to

$$\frac{\mu_0 \mu_N \mu_B g_N |g_e|}{\hbar^2} \left[\int \psi_{nlm'}(\vec{r})^* \left(\frac{3(\vec{S} \cdot \vec{r})(\vec{I} \cdot \vec{r}) - r^2(\vec{S} \cdot \vec{I})}{4\pi r^5} \right) \psi_{nlm}(\vec{r}) d^3r + \frac{2}{3}(\vec{S} \cdot \vec{I})|\psi_{n00}(\vec{0})|^2 \delta_{l0} \right]. \quad (1.18)$$

If $l = 0$ we have the spherically symmetric s orbitals, the only orbitals which are finite at the origin. Furthermore, it turns out that the first term in the integral vanishes in the $l = 0$ limit. It is not due to orthogonality, but the angular integral still exactly vanishes. To see this, we can write the components of \hat{r} in spherical

polar coordinates and then integrate:

$$\begin{aligned}
& \int_0^\pi \int_0^{2\pi} \sin \theta Y_0^{0*} [3(\vec{S} \cdot \hat{r})(\vec{I} \cdot \hat{r}) - (\vec{S} \cdot \vec{I})] Y_0^0 d\theta d\phi \\
&= |Y_0^0|^2 \int \sin \theta [3(\vec{S} \cdot \hat{r})(\vec{I} \cdot \hat{r}) - (\vec{S} \cdot \vec{I})] d\theta d\phi \\
&= |Y_0^0|^2 \int \sin \theta [3(S_x I_x \sin^2 \theta \cos^2 \phi + S_y I_y \sin^2 \theta \sin^2 \phi + S_z I_z \cos^2 \theta \\
&\quad + (S_x I_y + S_y I_x) \sin^2 \theta \sin \phi \cos \phi + (S_x I_z + S_z I_x) \sin \theta \cos \theta \cos \phi \\
&\quad + (S_y I_z + S_z I_y) \sin \theta \cos \theta \sin \phi) - \vec{S} \cdot \vec{I}] d\theta d\phi \\
&= |Y_0^0|^2 [S_x I_x + S_y I_y + S_z I_z - \vec{S} \cdot \vec{I}] = 0. \tag{1.19}
\end{aligned}$$

Therefore, for $l = 0$ we see that only the contact term contributes, just as in the classical case, and we can write down an expression for the effective spin-spin Hamiltonian:

$$\begin{aligned}
\hat{H}_{SI}^{\text{eff}} &= \frac{\mu_0 \mu_N \mu_B g_N |g_e|}{\hbar^2} |\psi_{n00}(\vec{0})|^2 \vec{S} \cdot \vec{I} \\
&= \frac{2\mu_0 \mu_N \mu_B g_N |g_e|}{3\hbar^2} \frac{Z_{\text{eff}}^3}{\pi n^3 a_0^3} \vec{S} \cdot \vec{I} = \frac{2}{3} \frac{E_0(n)}{\hbar^2} \vec{S} \cdot \vec{I} \equiv \frac{\alpha_{n00}^q}{\hbar^2} \vec{S} \cdot \vec{I}. \tag{1.20}
\end{aligned}$$

Here we have introduced the hyperfine structure constant for the s orbitals in the quantum limit, α_{n00}^q , but it turns out that this constant is identical to that of the classical limit: $\alpha_{n00}^q = \alpha_{n00}^c \equiv \alpha_{n00}$.

In the $l > 0$ limit, the contact term once again vanishes due to these orbitals

vanishing at the origin. In these cases, only the first term remains:

$$\begin{aligned}
\hat{H}_{SI}^{\text{eff}} &= \frac{\mu_0 \mu_N \mu_B g_N |g_e|}{\hbar^2} \int \psi_{nlm'}(\vec{r})^* \left(\frac{3(\vec{S} \cdot \vec{r})(\vec{I} \cdot \vec{r}) - r^2(\vec{S} \cdot \vec{I})}{4\pi r^5} \right) \psi_{nlm}(\vec{r}) d^3r \\
&= \frac{\mu_0 \mu_N \mu_B g_N |g_e|}{\hbar^2} \int \frac{|R_{nl}|^2}{4\pi r^3} r^2 dr \int \sin \theta Y_l^{m'*} (3(\vec{S} \cdot \hat{r})(\vec{I} \cdot \hat{r}) - (\vec{S} \cdot \vec{I})) Y_l^m d\theta d\phi \\
&= \frac{\mu_0 \mu_N \mu_B g_N |g_e|}{\hbar^2} \left\langle \frac{1}{4\pi r^3} \right\rangle \int \sin \theta Y_l^{m'*} (3(\vec{S} \cdot \hat{r})(\vec{I} \cdot \hat{r}) - (\vec{S} \cdot \vec{I})) Y_l^m d\theta d\phi \\
&= \frac{\mu_0 \mu_N \mu_B g_N |g_e|}{\hbar^2} \frac{(Z_{\text{eff}})^3}{2\pi a_0^3 l(l+1)(2l+1)n^3} \int \sin \theta Y_l^{m'*} (3(\vec{S} \cdot \hat{r})(\vec{I} \cdot \hat{r}) - (\vec{S} \cdot \vec{I})) Y_l^m d\theta d\phi.
\end{aligned} \tag{1.21}$$

The angular integral can be done by expanding \hat{r} in spherical polar coordinates as previously shown for the $l = 0$ case. However, this time it will not vanish and what is left will be a second-rank tensor involving \vec{L} , \vec{S} , and \vec{I} . Although more elegant methods exist, one sure-fire way to deduce the \vec{L} , \vec{S} , and \vec{I} dependence remaining after the integration is to express this tensor in the large Hilbert space of $\vec{L} \otimes \vec{S} \otimes \vec{I}$ and deduce its form by brute force. We propose $\hat{H}_{SI}^{\text{eff}}$ has the following form:

$$\hat{H}_{SI}^{\text{eff}} = a_l \vec{S} \cdot \vec{I} + b_l (\vec{L} \cdot \vec{I})(\vec{L} \cdot \vec{S}) + c_l (\vec{L} \cdot \vec{S})(\vec{L} \cdot \vec{I}).$$

It turns out that this is the correct form, for $l > 0$. Thus for s, p, d, and f orbitals we have the following effective Hamiltonians:

$$\begin{aligned}
l = 0 : \quad \hat{H}_{SI}^{\text{eff}} &= \frac{2}{3} \frac{E_0(n)}{\hbar^2} \vec{S} \cdot \vec{I} \\
l = 1 : \quad \hat{H}_{SI}^{\text{eff}} &= \frac{1}{12} \frac{E_0(n)}{\hbar^2} \left(\frac{4}{5} \vec{S} \cdot \vec{I} - \frac{6}{5} \frac{(\vec{L} \cdot \vec{I})(\vec{L} \cdot \vec{S}) + (\vec{L} \cdot \vec{S})(\vec{L} \cdot \vec{I})}{2} \right) \\
l = 2 : \quad \hat{H}_{SI}^{\text{eff}} &= \frac{1}{60} \frac{E_0(n)}{\hbar^2} \left(\frac{4}{7} \vec{S} \cdot \vec{I} - \frac{2}{7} \frac{(\vec{L} \cdot \vec{I})(\vec{L} \cdot \vec{S}) + (\vec{L} \cdot \vec{S})(\vec{L} \cdot \vec{I})}{2} \right) \\
l = 3 : \quad \hat{H}_{SI}^{\text{eff}} &= \frac{1}{168} \frac{E_0(n)}{\hbar^2} \left(\frac{8}{15} \vec{S} \cdot \vec{I} - \frac{2}{15} \frac{(\vec{L} \cdot \vec{I})(\vec{L} \cdot \vec{S}) + (\vec{L} \cdot \vec{S})(\vec{L} \cdot \vec{I})}{2} \right). \tag{1.22}
\end{aligned}$$

Finally, the quantum hyperfine couplings are defined as follows:

$$\langle m' | \hat{H}_{SI}^{\text{eff}} | m \rangle \equiv \frac{\alpha_{nlm,m'}^q}{\hbar^2} \hat{F}(\vec{S}, \vec{I})$$

where \hat{F} is some spin operator, composed of the electron spin and nuclear spin operators that are left over after integrating out spatial degrees of freedom.

At this point you may be wondering what the difference between \hat{H}_{SI} [Eq. (1.6)] and $\hat{H}_{SI}^{\text{eff}}$ [Eq. (1.22)] is in the quantum limit. Furthermore, since they lead to the same hyperfine couplings, you may be wondering whether they are redundant. The answer lies in what you plan to do. If you plan to work in the $|m_l, m_s\rangle$ basis then truly speaking either form will do. However, if you plan to work in the $|J, m_J\rangle$ basis then you must use $\hat{H}_{SI}^{\text{eff}}$, resisting the urge to evaluate the hyperfine couplings, and follow the procedure laid out in section 1.11. Otherwise, you will not be able to match your Hamiltonian to one which contains \vec{J} to first order.

1.6 Quantum Hyperfine Couplings in the Classical Limit

In the classical limit, \vec{S} and \vec{I} are classical vectors that point along the z-axis: $\vec{S} \equiv \hat{S}_z \hat{e}_z$ and $\vec{I} \equiv \hat{I}_z \hat{e}_z$. Thus, $\vec{S} \cdot \vec{I} = \hat{S}_z \hat{I}_z$ and $\frac{(\vec{L} \cdot \vec{I})(\vec{L} \cdot \vec{S}) + (\vec{L} \cdot \vec{S})(\vec{L} \cdot \vec{I})}{2} = \hat{L}_z^2 S_z I_z = m^2 S_z I_z$, for $m' = m$. In this limit, $\hat{H}_{SI}^{\text{eff}}$ simplifies to the classical result, in agreement with the previous derivations:

$$\begin{aligned} l = 0: \quad \hat{H}_{SI}^{\text{eff}} &= \frac{2}{3} \frac{E_0(n)}{\hbar^2} S_z I_z \equiv \frac{\alpha_{n00}^c}{\hbar^2} S_z I_z \\ l = 1: \quad \hat{H}_{SI}^{\text{eff}} &= \frac{1}{12} \left(\frac{4-6m^2}{5} \right) \frac{E_0(n)}{\hbar^2} S_z I_z \equiv \frac{\alpha_{n1m}^c}{\hbar^2} S_z I_z \\ l = 2: \quad \hat{H}_{SI}^{\text{eff}} &= \frac{1}{60} \left(\frac{4-2m^2}{7} \right) \frac{E_0(n)}{\hbar^2} S_z I_z \equiv \frac{\alpha_{n2m}^c}{\hbar^2} S_z I_z \\ l = 3: \quad \hat{H}_{SI}^{\text{eff}} &= \frac{1}{168} \left(\frac{8-2m^2}{15} \right) \frac{E_0(n)}{\hbar^2} S_z I_z \equiv \frac{\alpha_{n3m}^c}{\hbar^2} S_z I_z \end{aligned}$$

1.7 The Effective Hamiltonian due to the Coupling of the Electron Angular Momentum and the Nuclear Spin

The energy due to the coupling of the magnetic moment of the nucleus to the magnetic field created by the orbital angular momentum of the electron is given by the Hamiltonian

$$\hat{H}_{LI} = -\vec{m}_I \cdot \vec{B}_L(\vec{0}).$$

The magnetic field at \vec{r} due to the electron's orbital angular momentum is given by the Biot-Savart law:

$$\vec{B}_L(\vec{r}) = \frac{\mu_0}{4\pi} \int \vec{J}(\vec{R}) \times \frac{\vec{r}-\vec{R}}{|\vec{r}-\vec{R}|^3} d^3R$$

However, only the vector value of the magnetic field at the nucleus, taken to be at the origin, contributes to the hamiltonian. Setting, $\vec{r} = \vec{0}$,

$$\vec{B}_L(\vec{0}) = -\frac{\mu_0}{4\pi} \int \vec{J}(\vec{R}) \times \frac{\vec{R}}{R^3} d^3R$$

We can write the electric current density, $\vec{J}(\vec{R})$, in terms of the quantum mechanical probability density: $\vec{J}(\vec{R}) = q\vec{j}(\vec{R}) = -e\vec{j}(\vec{R})$. In addition, the quantum mechanical probability density is defined in terms of the wavefunction: $\vec{j} = \frac{\hbar}{2m_e i}(\psi^* \nabla \psi - \psi \nabla \psi^*)$. Thus, the electric current density can also be defined in terms of the wavefunction by:

$$\vec{J} = \frac{-e\hbar}{2m_e i}(\psi^* \nabla \psi - \psi \nabla \psi^*).$$

Furthermore, we can define $\vec{B}_L(\vec{0})$ in terms of \vec{L} after some manipulation:

$$\begin{aligned} \vec{J} \times (-)\vec{r} &= \vec{r} \times \vec{J} \\ &= \vec{r} \times \left[\frac{-e\hbar}{2m_e i}(\psi^* \nabla \psi - \psi \nabla \psi^*) \right] \\ &= \vec{r} \times \left[\frac{-e}{2m_e}(\psi^* \vec{p} \psi - \psi \vec{p} \psi^*) \right] \end{aligned}$$

$$= \frac{-e}{2m_e} (\psi^* \vec{L} \psi - \psi \vec{L} \psi^*)$$

Thus, we can combine all these factors to obtain an expression for the magnetic field at the nucleus in terms of \vec{L} due to the orbital angular momentum of the electrons:

$$\vec{B}_L(\vec{0}) = -\frac{\mu_0 e}{8\pi m_e} \int (\psi^* \vec{L} \psi - \psi \vec{L} \psi^*) \frac{1}{r^3} d^3 r$$

If ψ is a hydrogenic wavefunction such as $\psi = \psi_{nlm}$, then $\vec{B}_L(\vec{0})$ simplifies to:

$$\begin{aligned} \vec{B}_L(\vec{0}) &= -\frac{\mu_0 e}{8\pi m_e} \int (\psi_{nlm}^* \vec{L} \psi_{nlm} - \psi_{nlm} \vec{L} \psi_{nlm}^*) \frac{1}{R^3} d^3 R \\ &= -\frac{\mu_0 e}{8\pi m_e} \int \frac{1}{r} R_{nl}^2 dr \int \sin \theta (Y_l^{m*} \vec{L} Y_l^m - Y_l^m \vec{L} Y_l^{m*}) d\theta d\phi \\ &= -\frac{\mu_0 e}{8\pi m_e} \langle \frac{1}{r^3} \rangle \int \sin \theta (Y_l^{m*} \vec{L} Y_l^m - Y_l^m \vec{L} Y_l^{m*}) d\theta d\phi \\ &= -\frac{m_l \mu_0 \mu_B Z_{\text{eff}}^3}{\pi n^3 a_0^3 l(l+1)(2l+1)} \hat{e}_z = -\frac{\mu_0 \mu_B Z_{\text{eff}}^3}{\pi n^3 a_0^3 l(l+1)(2l+1) \hbar} \langle \hat{L}_z \rangle \hat{e}_z \equiv -\frac{B_{nl}}{\hbar} \langle \hat{L}_z \rangle \hat{e}_z, \end{aligned}$$

$$\text{where } B_{nl} = \frac{\mu_0 \mu_B Z_{\text{eff}}^3}{\pi n^3 a_0^3 l(l+1)(2l+1)} \approx \frac{Z_{\text{eff}}^3}{n^3 l(l+1)(2l+1)} \times 25 \text{ Tesla.}$$

However, more generally speaking ψ may be a superposition state of Hydrogenic wavefunctions with the same n and l . In this case, $\vec{B}_L(\vec{0})$ simplifies to:

$$\vec{B}_L(\vec{0}) = -\frac{B_{nl}}{\hbar} \langle \vec{L} \rangle .$$

Furthermore, since matrix elements of \hat{L}_x , \hat{L}_y , and \hat{L}_z contribute to the respective x, y, or z components of the magnetic field, we may define $\vec{B}_L(\vec{0})$ as an operator proportional to \vec{L} ;

$$\hat{B}_L(0) \equiv -\frac{B_{nl}}{\hbar} \vec{L}$$

Now that we have derived the magnetic field due to the orbital angular momentum of the electron, we are ready to write down the energy due to its coupling with the nuclear magnetic moment:

$$\hat{H}_{LI} = -\vec{m}_I \cdot \hat{B}_L(\vec{0}), \quad \vec{m}_I = \frac{g_N \mu_N}{\hbar} \vec{I}. \quad (1.23)$$

Finally, we may write down the Hamiltonian describing the coupling of the electron orbital angular momentum to the nuclear magnetic moment in terms of \vec{L} and \vec{I} :

$$\hat{H}_{LI} = \frac{g_N \mu_N B_{nl}}{\hbar^2} \vec{L} \cdot \vec{I} \equiv \frac{\beta_{nl}}{\hbar^2} \vec{L} \cdot \vec{I}.$$

1.8 The Hyperfine Splitting in Hydrogen 1s

The ground state electronic configuration of Hydrogen is $1s^1$, or equivalently $|100\rangle$ in the $|nlm\rangle$ basis. This spatial part of the wavefunction is absent of any orbital angular momentum, and so the total energy can simply be given by $\langle \hat{H}_{SI} \rangle$. As before, we will first take the expectation with respect to the spatial part of the wavefunction, ψ_{100} , in effect integrating out all spatial degrees of freedom. This leaves behind the spin part of the Hamiltonian only, which we will be able to write as a 4x4 matrix since $S = I = \frac{1}{2}$ in Hydrogen.

Recalling our previous relation for spherically symmetric states, we can immediately write down the expression for the $n = 1$ case, with $g_N \rightarrow g_p$ and $Z_{\text{eff}} \rightarrow 1$:

$$\langle 100 | \hat{H}_{SI} | 100 \rangle = \frac{2\mu_0 \mu_N \mu_B g_p |g_e|}{3\hbar^2} \left| \psi_{100}(\vec{0}) \right|^2 \vec{S} \cdot \vec{I} = \frac{\alpha_{100}}{\hbar^2} \vec{S} \cdot \vec{I}$$

Since $S = I = \frac{1}{2}$, each spin has two possible states and $\vec{S} \cdot \vec{I}$ can be written as a 4x4 matrix in the basis of $|m_s m_I\rangle$ states:

$$\langle 100 | \hat{H}_{SI} | 100 \rangle = \frac{\alpha_{100}}{\hbar^2} \begin{pmatrix} \frac{1}{4} & 0 & 0 & 0 \\ 0 & -\frac{1}{4} & \frac{1}{2} & 0 \\ 0 & \frac{1}{2} & -\frac{1}{4} & 0 \\ 0 & 0 & 0 & \frac{1}{4} \end{pmatrix}$$

This matrix has four eigenvectors: $|\frac{1}{2}, \frac{1}{2}\rangle$, $|\frac{1}{2}, -\frac{1}{2}\rangle$, $|\frac{1}{\sqrt{2}}(|\frac{1}{2}, -\frac{1}{2}\rangle + |-\frac{1}{2}, \frac{1}{2}\rangle)$ and $\frac{1}{\sqrt{2}}(|\frac{1}{2}, -\frac{1}{2}\rangle - |-\frac{1}{2}, \frac{1}{2}\rangle)$, the first three of which are degenerate. For simplicity, we define $|\Psi^+\rangle \equiv \frac{1}{\sqrt{2}}(|\frac{1}{2}, -\frac{1}{2}\rangle + |-\frac{1}{2}, \frac{1}{2}\rangle)$ and $|\Psi^-\rangle \equiv \frac{1}{\sqrt{2}}(|\frac{1}{2}, -\frac{1}{2}\rangle - |-\frac{1}{2}, \frac{1}{2}\rangle)$. These

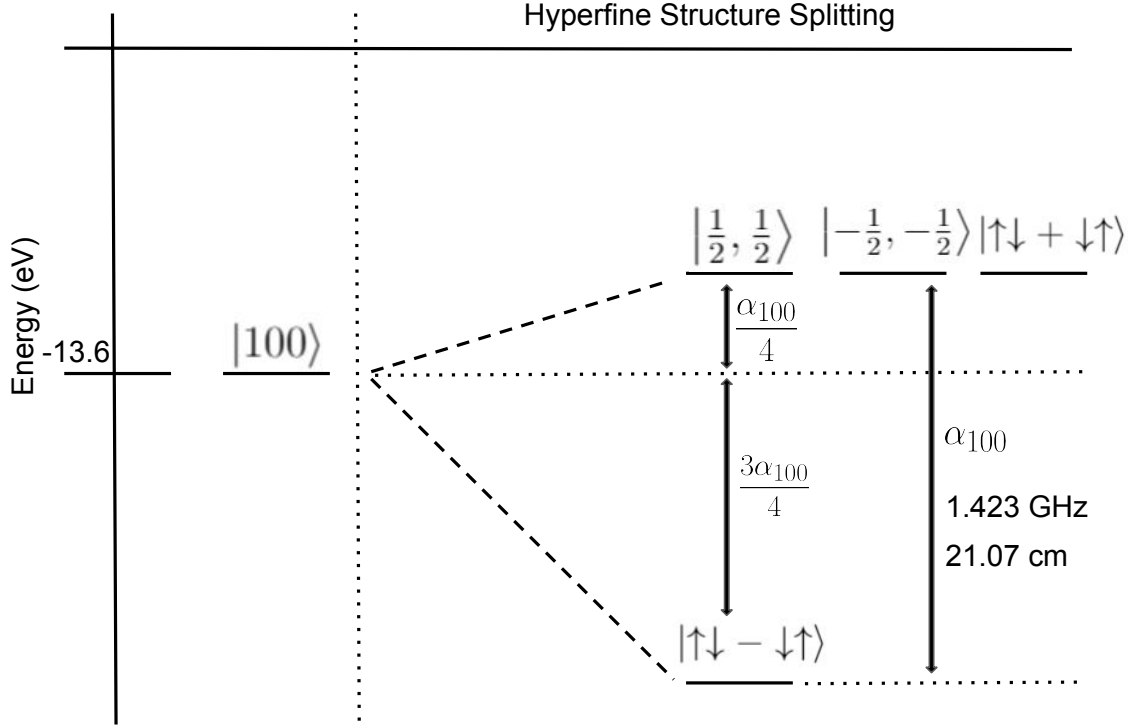


Figure 1.1: Hyperfine splitting diagram of Hydrogen 1s

happen to be two of the four Bell states, in which the electron spin and nuclear spin are maximally entangled.

Since $E_{SI} = -\vec{m}_e \cdot \vec{B}_I \propto \vec{S} \cdot \vec{B}_I \propto \vec{S} \cdot \vec{I}$, the ground state configuration prefers having the nuclear and electronic spins anti-parallel. Although both $|\Psi^+\rangle$ and $|\Psi^-\rangle$ appear to meet this condition, only $|\Psi^-\rangle$ has all components of \vec{S} and \vec{I} anti-parallel. Thus, $|\Psi^-\rangle$ is the singlet ground state, while the triplet states are the excited states. The triplet states are degenerate with energy $E_{triplet} = \frac{1}{4}\alpha_{100}$ while the singlet state is of lower energy, $E_{singlet} = -\frac{3}{4}\alpha_{100}$, as shown in Fig. 1.1. Thus, the hyperfine splitting is given by the difference between these energies: $\Delta E = E_{triplet} - E_{singlet} = \alpha_{100} = 5.884 \mu\text{eV}$. This energy splitting corresponds to the famous 21-cm spectral line^{4,5} and our calculation closely matches this at 21.07 cm.

1.9 The Hyperfine Stark Effect in Hydrogen 1s

The presence of an external electric field, taken to be along the z-axis, perturbs the ground state wavefunction via the quadratic Stark effect⁶, and in turn we expect some impact on the hyperfine splitting. This effect is referred to as the hyperfine Stark effect. In this section, we use two methods to calculate the first order correction to the ground state wavefunction in order to calculate the hyperfine Stark effect in hydrogen. However, since we neglect fine structure effects, this section should be treated more as an exercise to get an order-of-magnitude estimate of the hyperfine Stark effect in hydrogen 1s.

The first method is time-independent perturbation theory, where the perturbing potential is assumed to be at least an order of magnitude weaker than the bare Hamiltonian. In SI units, the Hamiltonian for a hydrogenic atom placed in a static electric field along the positive z-axis is given by:

$$\hat{H} = \frac{\hat{p}^2}{2m_e} - \frac{e^2}{4\pi\epsilon_0 r} + e|\vec{E}|\hat{z} = \frac{-\hbar^2}{2m_e}\nabla^2 - \frac{e^2}{4\pi\epsilon_0 r} + e|\vec{E}|r \cos \theta$$

Thus, the time independent Schrödinger equation becomes:

$$\left[\frac{-\hbar^2}{2m_e}\nabla^2 - \frac{e^2}{4\pi\epsilon_0 r} + e|\vec{E}|r \cos \theta\right]\psi_n = E_n\psi_n$$

In the ground state of hydrogen, the bare Hamiltonian has a well-known energy of -13.6 eV. Even for extreme electric fields such as $|\vec{E}| \sim 10^8$ V m⁻¹, the matrix elements of the energy due to the electric field are of the order of $e|\vec{E}|a_0$, which is several orders of magnitude lower in energy than that of the bare Hamiltonian. Therefore, the contribution to the Hamiltonian due to the external electric field can be treated as a perturbation, and we can expect that time-independent perturbation theory will provide a very good first-order correction to the wavefunction and energy.

In a standard way of deriving the order-by-order perturbation theory differential equations, we introduce a small perturbation parameter, $\lambda < 1$, to track the relative strength of each term. From here we make a series of definitions, making use of the perturbation parameter:

$$\hat{H} = \hat{H}^0 + \lambda \hat{H}^1, \text{ where } \hat{H}^0 = \frac{-\hbar^2}{2m_e} \nabla^2 - \frac{e^2}{4\pi\epsilon_0 r} \text{ and } \hat{H}^1 = -e|\vec{E}|r \cos \theta$$

Furthermore, it is standard to expand the wavefunction and energy in a power series in λ :

$$\psi_n = \sum_{i=0}^{\infty} \lambda^i \phi_n^{(i)} \text{ and } E_n = \sum_{j=0}^{\infty} \lambda^j E_n^{(j)}$$

where a (i) or (j) index refers to the i^{th} or j^{th} order correction wavefunction or energy, respectively. Here it is understood that the zeroth-order correction terms satisfy the Schrödinger equation of the bare Hamiltonian: $\hat{H}^0 \phi_n^{(0)} = E_n^0 \phi_n^{(0)}$, where $\phi_n^{(0)}$ refers to the $|nlm\rangle$ states projected in position space. Finally, by substituting all of these terms into the Schrödinger equation, we obtain:

$$(\hat{H}^0 + \lambda \hat{H}^1) \sum_{i=0}^{\infty} \lambda^i \phi_n^{(i)} = \sum_{i=0}^{\infty} \sum_{j=0}^{\infty} \lambda^{i+j} E_n^{(j)} \phi_n^{(i)}$$

We now have an infinite number of differential equations, one for each power in λ . However, the main contributions to the wavefunction are given by only the zeroth-order and first-order corrections, while higher order corrections are negligible in comparison. The $\lambda = 0$ differential equation is just the Schrödinger equation of \hat{H}_0 , and these solutions and corresponding energies are well-known. Therefore, we need only focus on the $\lambda = 1$ differential equation:

$$\hat{H}^0 \phi_n^{(1)} + \hat{H}^1 \phi_n^{(0)} = E_n^{(0)} \phi_n^{(1)} + E_n^{(1)} \phi_n^{(0)}$$

By multiplying both sides of this equation with $\phi_n^{(0)*}$ and integrating over all space, we obtain a formula for the first-order energy shift:

$$E_n^{(1)} = \int [\phi_n^{(0)*}]^* \hat{H}^1 \phi_n^{(0)} d^3r$$

However, in the ground state this integral is proportional to $\int_{\theta=0}^{\theta=\pi} \sin \theta \cos \theta d\theta = 0$, thus, $E_1^{(1)} = 0$. In a similar way, by multiplying both sides of the $\lambda = 1$ differential equation by $\phi_k^{(0)*}$, for $k \neq n$, and integrating over all space, we obtain a formula for the first order correction to the wavefunction:

$$\phi_n^{(1)} = \sum_{k \neq n}^{\infty} \frac{\int \phi_k^{(0)*} \hat{H}^1 \phi_n^{(0)} d^3r}{E_n^{(0)} - E_k^{(0)}} \phi_k^{(0)} \equiv \sum_{k \neq n}^{\infty} C_k \phi_k^{(0)}$$

Thus, the first order correction to the wavefunction can be expanded in the basis of the eigenstates of the bare Hamiltonian, which are the well-known hydrogenic wavefunctions. We can reduce the number of terms in this sum by recalling the selection rules of \hat{z} :

$$\langle n'l'm' | \hat{z} | nlm \rangle \neq 0 \text{ for } \Delta l = \pm 1 \text{ and } \Delta m = 0$$

For the ground state, $l = m = 0$, which restricts $l' = \pm 1$ and $m' = 0$. Therefore, the first order correction to $|100\rangle$ can only be expanded in $|k10\rangle$ states:

$$\phi_1^{(1)} = \sum_{k=2}^{\infty} \frac{\langle k10 | \hat{H}^1 | 100 \rangle}{E_1^{(0)} - E_k^{(0)}} \psi_{k10} = e |\vec{E}| \sum_{k=2}^{\infty} \frac{\int \phi_k^{(0)*} r \cos \theta \psi_{100} d^3r}{E_n^{(0)} - E_k^{(0)}} \psi_{k10}$$

It turns out that the largest coefficients of $\psi_{k10} \sim 10^{-10} |\vec{E}|$ and so it is sufficient to keep only the first term in the sum, even in the case of extreme external electric fields. Finally, the first order corrected normalized wavefunction is given by:

$$\psi_{PT} \simeq \frac{1}{\sqrt{1 + \left(\frac{512\sqrt{2}e|\vec{E}|a_0}{729E_1^{(0)}}\right)^2}} [\psi_{100} + \left(\frac{512\sqrt{2}e|\vec{E}|a_0}{729E_1^{(0)}}\right) \psi_{210}] \equiv \frac{1}{\sqrt{1 + \gamma_{PT}^2}} [\psi_{100} + \gamma_{PT} \psi_{210}]$$

The second method we use to calculate the first order correction to the ground state wavefunction is called the Dalgarno-Lewis method⁷, which produces an exact analytic solution. The starting point is the following equation from the perturbation theory method:

$$\hat{H}^0 \phi_n^{(1)} + \hat{H}^1 \phi_n^{(0)} = E_n^{(0)} \phi_n^{(1)} + E_n^{(1)} \phi_n^{(0)}$$

However, we are concerned with the first order correction to the ground state $n = 1$. Thus, $\phi_1^{(0)} \equiv \psi_{100}$ and $E_1^{(1)} = 0$ as previously derived. The next step is to rearrange the above equation in the following way:

$$[\hat{H}^0 - E_1^{(0)}] \phi_1^{(1)} = -\hat{H}^1 \psi_{100}(r)$$

We now have a differential equation for the first order correction wavefunction to the ground state, with the perturbing Hamiltonian acting on the ground state wavefunction itself as a forcing. Substituting \hat{H}^0 and \hat{H}^1 into the differential equation we obtain:

$$\left[\frac{-\hbar^2}{2m_e} \nabla^2 - \frac{e^2}{4\pi\epsilon_0 r} - E_1^{(0)} \right] \phi_1^{(1)} = e |\vec{E}| r \cos \theta \psi_{100}(r)$$

But $\cos \theta$ is proportional to the Y_1^0 spherical harmonic, and so the forcing term is proportional to $|\vec{E}| Y_1^0$. Therefore, we guess that $\phi_1^{(1)}$ may have the same symmetry. Specifically, we let $\phi_1^{(1)} = |\vec{E}| F(r) Y_1^0(\theta, \phi)$:

$$\left[\frac{-\hbar^2}{2m_e} \nabla^2 - \frac{e^2}{4\pi\epsilon_0 r} - E_1^{(0)} \right] F(r) Y_1^0(\theta, \phi) = e \sqrt{\frac{4\pi}{3}} r \psi_{100}(r) Y_1^0(\theta, \phi)$$

For the time being it is useful to switch to atomic units for the sake of solving this differential equation:

$$\left[\frac{-1}{2} \tilde{\nabla}^2 - \frac{1}{\tilde{r}} + \frac{1}{2} \right] \tilde{F}(\tilde{r}) Y_1^0(\theta, \phi) = \sqrt{\frac{4\pi}{3}} \tilde{r} \tilde{\psi}_{100}(\tilde{r}) Y_1^0(\theta, \phi)$$

From this point on the tildes will be dropped for clarity, but it is understood that we are still in atomic units. Since we have written all angular functions in terms of the spherical harmonics, it makes sense to write ∇^2 in spherical polar coordinates. The differential equation now becomes:

$$\frac{-1}{2} \left[\frac{\partial_r (r^2 \partial_r F)}{r^2} Y_1^0 + \frac{\partial_\theta (\sin \theta \partial_\theta Y_1^0)}{r^2 \sin \theta} F \right] - \frac{FY_1^0}{r} + \frac{FY_1^0}{2} = \sqrt{\frac{4\pi}{3}} r \psi_{100} Y_1^0$$

To separate this partial differential equation into two ordinary differential equations, we simply multiply by $\frac{r^2}{F(r)Y_1^0}$:

$$\frac{-1}{2} \left[\frac{\partial_r(r^2 \partial_r F)}{F} + \frac{\partial_\theta(\sin \theta \partial_\theta Y_1^0)}{\sin \theta Y_1^0} \right] - r + \frac{r^2}{2} = \sqrt{\frac{4\pi}{3}} \frac{r^3 \psi_{100}}{F}$$

As expected, all terms are now functions of only one variable. Note that the second term has no dependence on r . If we view the above line as an ordinary differential equation in r , the second term must be a constant with respect to r . Since the spherical harmonics are eigenfunctions of the Laplacian, we expect this constant to equal $-l(l+1) = -2$, and indeed it does if one simplifies the derivatives. We now have an ordinary differential equation for $F(r)$, and we may multiply through by $F(r)$ and simplify to obtain:

$$F'' + \frac{2}{r}F' - \left(1 - \frac{2}{r} + \frac{2}{r^2}\right)F = \frac{-4}{\sqrt{3}}r e^{-r}$$

Miraculously, this differential equation has an analytical solution:

$$F(r) = \frac{3+6r+6r^2+4r^3+2r^4}{2\sqrt{3}r^2} e^{-r} + C_1 \frac{e^r}{r^2} - C_2 \frac{1+2r+2r^2}{4r^2} e^{-r}$$

Applying the boundary conditions, $F(r \rightarrow \infty) \rightarrow 0$ and $F(r \rightarrow 0) = \text{finite}$, we obtain:

$$\phi_1^1 = |\vec{E}| F(r) Y_1^0 = \frac{|\vec{E}|}{\sqrt{3}} (2r + r^2) e^{-r} Y_1^0$$

However, this is in atomic units. By restoring SI units we obtain:

$$\phi_1^1 = \sqrt{\frac{1}{a_0^3}} \left(\frac{e|\vec{E}a_0}{4\sqrt{3}E_1} \right) \left(2\left(\frac{r}{a_0}\right) + \left(\frac{r}{a_0}\right)^2 \right) e^{-r/a_0} Y_1^0$$

where E_1 is the energy of the ground state of \hat{H}_0 . Finally, the first-order corrected normalized wavefunction is given by:

$$\psi_{DL} = \frac{1}{\sqrt{1 + \frac{43}{128} \left(\frac{e|\vec{E}|a_0}{E_1} \right)^2}} \left[\psi_{100} + \sqrt{\frac{1}{a_0^3}} \left(\frac{e|\vec{E}a_0}{4\sqrt{3}E_1} \right) \left(2\left(\frac{r}{a_0}\right) + \left(\frac{r}{a_0}\right)^2 \right) e^{-r/a_0} Y_1^0 \right]$$

$$\equiv \lambda_{DL}[\psi_{100} + \gamma_{DL}F(r)Y_1^0]$$

where $\gamma_{DL} \equiv \frac{e|\vec{E}|a_0}{4\sqrt{3}E_1}$ and $F(r) \equiv \sqrt{\frac{1}{a_0^3}}(2(\frac{r}{a_0}) + (\frac{r}{a_0})^2)e^{-r/a_0}$.

In order to calculate hyperfine splittings, we will first take the expectation value of \hat{H}_{SI} with respect to the spatial states perturbed by the external electric field, ψ_{PT} or ψ_{DL} . As before this will leave behind the spin part of the Hamiltonian only, which can be written as a 4x4 matrix:

$$\langle \psi_{PT} | \hat{H}_{SI} | \psi_{PT} \rangle$$

$$\begin{aligned} &= \frac{1}{1+\gamma_{PT}^2} [\langle \psi_{100} | \hat{H}_{SI} | \psi_{100} \rangle + \gamma_{PT}^2 \langle \psi_{210} | \hat{H}_{SI} | \psi_{210} \rangle + 2\gamma_{PT} \langle \psi_{100} | \hat{H}_{SI} | \psi_{210} \rangle] \\ &= \frac{1}{(1+\gamma_{PT}^2)\hbar^2} [\alpha_{100}\vec{S} \cdot \vec{I} - \alpha_{210}\gamma_{PT}^2(\vec{S} \cdot \vec{I} - 3\hat{S}_z\hat{I}_z) + 0] \end{aligned}$$

$$\text{where } \alpha_{210} \equiv \langle \psi_{210} | \hat{H}_{SI} | \psi_{210} \rangle = \frac{\mu_0\mu_N\mu_B g_p |g_e|}{240\pi a_0^3}$$

$$\begin{aligned} &= \frac{1}{(1+\gamma_{PT}^2)\hbar^2} [(\alpha_{100} - \alpha_{210}\gamma_{PT}^2)\vec{S} \cdot \vec{I} + 3\alpha_{210}\gamma_{PT}^2\hat{S}_z\hat{I}_z] \\ &\doteq \frac{1}{(1+\gamma_{PT}^2)} \begin{pmatrix} \frac{+\alpha_{100}+2\alpha_{210}\gamma_{PT}^2}{4} & 0 & 0 & 0 \\ 0 & \frac{-\alpha_{100}-2\alpha_{210}\gamma_{PT}^2}{4} & \frac{\alpha_{100}-\alpha_{210}\gamma_{PT}^2}{2} & 0 \\ 0 & \frac{\alpha_{100}-\alpha_{210}\gamma_{PT}^2}{2} & \frac{-\alpha_{100}-2\alpha_{210}\gamma_{PT}^2}{4} & 0 \\ 0 & 0 & 0 & \frac{\alpha_{100}+2\alpha_{210}\gamma_{PT}^2}{4} \end{pmatrix} \end{aligned}$$

$$\langle \psi_{DL} | \hat{H}_{SI} | \psi_{DL} \rangle$$

$$\begin{aligned} &= \lambda_{DL}^2 [\langle \psi_{100} | \hat{H}_{SI} | \psi_{100} \rangle + \gamma_{DL}^2 \langle F(r)Y_1^0 | \hat{H}_{SI} | F(r)Y_1^0 \rangle + 2\gamma_{DL} \langle \psi_{100} | \hat{H}_{SI} | F(r)Y_1^0 \rangle] \\ &= \frac{\lambda_{DL}^2}{\hbar^2} [\alpha_{100}\vec{S} \cdot \vec{I} - \alpha_{DL}\gamma_{DL}^2(\vec{S} \cdot \vec{I} - 3\hat{S}_z\hat{I}_z) + 0] \end{aligned}$$

$$\text{where } \alpha_{DL} \equiv \langle F(r)Y_1^0 | \hat{H}_{SI} | F(r)Y_1^0 \rangle = \frac{19\mu_0\mu_N\mu_B g_p |g_e|}{80\pi a_0^3}$$

$$= \frac{\lambda_{DL}^2}{\hbar^2} [(\alpha_{100} - \alpha_{DL}\gamma_{DL}^2)\vec{S} \cdot \vec{I} + 3\alpha_{DL}\gamma_{DL}^2\hat{S}_z\hat{I}_z]$$

$$\doteq \lambda_{DL}^2 \begin{pmatrix} \frac{\alpha_{100}+2\alpha_{DL}\gamma_{DL}^2}{4} & 0 & 0 & 0 \\ 0 & \frac{-\alpha_{100}-2\alpha_{DL}\gamma_{DL}^2}{4} & \frac{\alpha_{100}-\alpha_{DL}\gamma_{DL}^2}{2} & 0 \\ 0 & \frac{\alpha_{100}-\alpha_{DL}\gamma_{DL}^2}{2} & \frac{-\alpha_{100}-2\alpha_{DL}\gamma_{DL}^2}{4} & 0 \\ 0 & 0 & 0 & \frac{\alpha_{100}+2\alpha_{DL}\gamma_{DL}^2}{4} \end{pmatrix}$$

Both of these matrices are of the same form and, as expected, they have the same eigenvalues: $|\frac{1}{2}, \frac{1}{2}\rangle$, $|\frac{1}{2}, -\frac{1}{2}\rangle$, $\frac{1}{\sqrt{2}}(|\frac{1}{2}, -\frac{1}{2}\rangle + |-\frac{1}{2}, \frac{1}{2}\rangle)$ and $\frac{1}{\sqrt{2}}(|\frac{1}{2}, -\frac{1}{2}\rangle - |-\frac{1}{2}, \frac{1}{2}\rangle)$. These are also the same eigenvectors as in the zero-field limit. However, the previously degenerate triplet excited states now experience some splitting due to the external electric field.

From perturbation theory we obtain:

$$E_{|\frac{1}{2}, \frac{1}{2}\rangle} = E_{|\frac{1}{2}, -\frac{1}{2}\rangle} = \frac{\alpha_{100}+2\alpha_{210}\gamma_{PT}^2}{4(1+\gamma_{PT}^2)}, E_+ = \frac{\alpha_{100}-4\alpha_{210}\gamma_{PT}^2}{4(1+\gamma_{PT}^2)}, \text{ and } E_- = \frac{-3\alpha_{100}}{4(1+\gamma_{PT}^2)}$$

From the Dalgarno-Lewis method we obtain:

$$E_{|\frac{1}{2}, \frac{1}{2}\rangle} = E_{|\frac{1}{2}, -\frac{1}{2}\rangle} = \frac{\lambda_{DL}^2(\alpha_{100}+2\alpha_{DL}\gamma_{DL}^2)}{4}, E_+ = \frac{\lambda_{DL}^2(\alpha_{100}-4\alpha_{DL}\gamma_{DL}^2)}{4}, \text{ and } E_- = -\lambda_{DL}^2 \frac{3\alpha_{100}}{4}$$

The energy of each state is of the same form, whether the wavefunction was calculated using perturbation theory or the Dalgarno-Lewis method, and in the presence of an external electric field the previously degenerate triplet splits into a doublet. This is shown in Fig. 1.2, where we have also shown the second-order energy shift's quadratic dependence on the electric field.

The emergent triplet state splitting is given by $\Delta E = E_{|\frac{1}{2}, \frac{1}{2}\rangle} - E_+ = \frac{3\alpha_{210}\gamma_{PT}^2}{2(1+\gamma_{PT}^2)}$ or $\frac{3}{2}\alpha_{DL}\gamma_{DL}^2\lambda_{DL}^2$. These expressions evaluate to 8.2 feV and 9.9 feV, frequencies of 2.0 Hz and 2.4 Hz, or wavelengths of 150 megameters or 125 megameters, respectively for extreme electric fields on the order of $\sim 10^8 \frac{V}{m}$. However, it is worth noting that these splittings are not completely accurate since we have neglected the fine

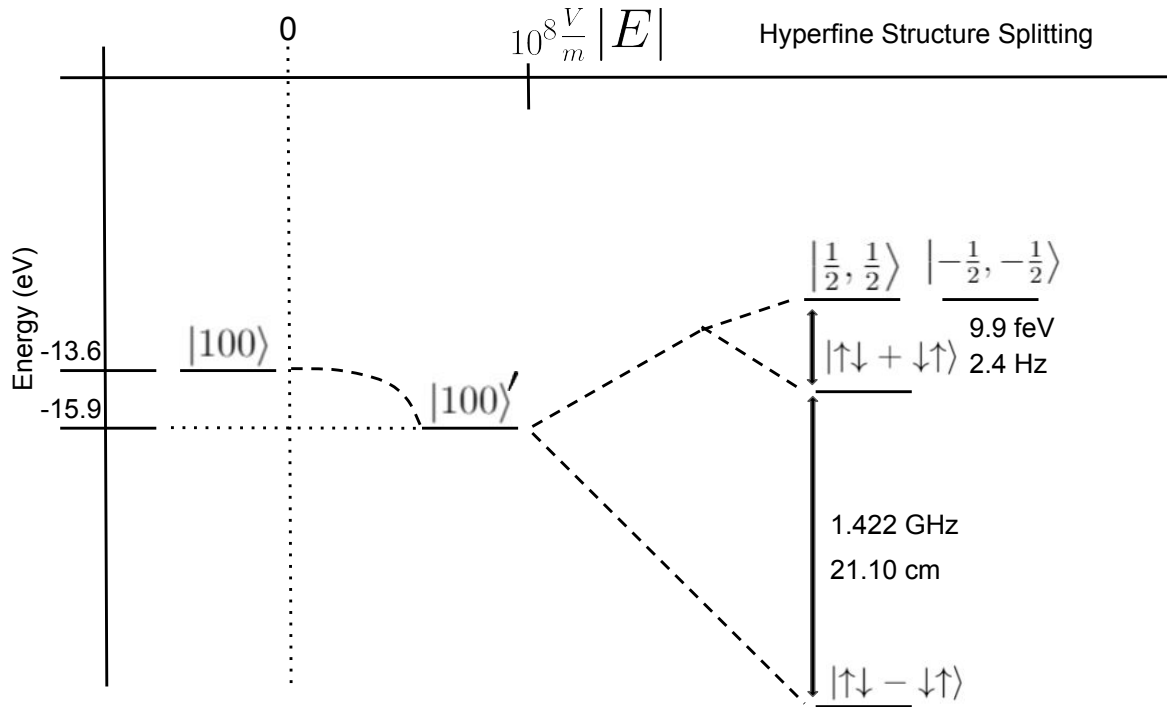


Figure 1.2: Hyperfine Stark effect splitting diagram of Hydrogen 1s

structure from the beginning. Furthermore, the splitting between $|\Psi^+\rangle$ and $|\Psi^-\rangle$ is relatively unchanged, regardless of the external electric field strength, as the two energy levels shift to lower energy by more or less the same amount. This splitting corresponds to $5.88 \mu\text{eV}$, 1.422 GHz , or 21.10 cm for extreme electric fields on the order of $\sim 10^8 \frac{\text{V}}{\text{m}}$, which is nearly equal to the splitting in the zero-field limit.

1.10 The Degenerate Hyperfine Stark Effect in Hydrogen $|2lm\rangle$

In this section, we use time independent degenerate perturbation theory to first order to determine the effect of an external electric field, taken to be along the z axis, on the $n = 2$ electronic states. Then we calculate the hyperfine splitting of these perturbed states. However, since we again neglect fine structure effects, this section should be

treated more as an exercise to get an order of magnitude estimate of the hyperfine Stark effect in Hydrogen 2s.

In first order time independent (non-degenerate) perturbation theory, it is assumed that the state being perturbed is not degenerate with any other states. In this case, the first order energy splitting is given by the expectation value of the perturbation Hamiltonian with respect to the eigenstates of the bare Hamiltonian. However, the $n = 2$ states of Hydrogen, $|200\rangle$ and $|21m\rangle$, are degenerate in the bare Hamiltonian and so all of these states need to be treated on an equal footing. Therefore, instead of a single expectation value, we construct the matrix of the perturbing Hamiltonian in the Hilbert space of these states. The first order energy corrections will be the eigenvalues of this matrix, and the first order corrected eigenstates will be eigenvectors.

Using the same notation as before, the perturbing Hamiltonian due to an external electric field along the z direction is given by:

$$\hat{H}^1 = -e|\vec{E}|\hat{z} = -e|\vec{E}|r \cos \theta$$

Matrix elements of \hat{H}^1 , H_{ij} , are given by the following integrals:

$$H_{ij} = -e|\vec{E}| \int \psi_i(\vec{r})^* r \cos \theta \psi_j(\vec{r}) d^3r$$

Where $\psi_i(\vec{r})^*$ stands for $\psi_{200}(\vec{r})^*$, $\psi_{210}(\vec{r})^*$, $\psi_{211}(\vec{r})^*$, or $\psi_{21-1}(\vec{r})^*$ while $\psi_j(\vec{r})$ stands for $\psi_{200}(\vec{r})$, $\psi_{210}(\vec{r})$, $\psi_{211}(\vec{r})$, or $\psi_{21-1}(\vec{r})$. In this Hilbert space, \hat{H}^1 takes the following form:

$$\langle 2l'm' | \hat{H}^1 | 2lm \rangle \doteq \frac{3e|\vec{E}|a_0}{Z_{\text{eff}}} \begin{pmatrix} 0 & 1 & 0 & 0 \\ 1 & 0 & 0 & 0 \\ 0 & 0 & 0 & 0 \\ 0 & 0 & 0 & 0 \end{pmatrix}$$

Where, the only surviving matrix elements are between $|200\rangle$ and $|210\rangle$. We can see that the $|211\rangle$ and $|21-1\rangle$ states remain unchanged by the external electric field, while the $|200\rangle$ and $|210\rangle$ states will couple in equal amounts. Thus, it is not surprising that the eigenvectors of this matrix are $|211\rangle$, $|21-1\rangle$, and $\frac{1}{\sqrt{2}}(|200\rangle \pm |210\rangle)$.

Next, we will calculate the hyperfine splitting of this last eigenvector by taking the expectation value of \hat{H}_{HF} with respect to this state, leaving the spin states to be determined later. Let $|\phi\rangle \equiv \frac{1}{\sqrt{2}}(|200\rangle + \lambda|210\rangle)$, where $\lambda = \pm 1$.

$$\begin{aligned} & \langle \phi | \hat{H}_{HF} | \phi \rangle \\ &= \frac{1}{2}([\langle 200 | + \lambda \langle 210 |] \hat{H}_{SI} [|200\rangle + \lambda |210\rangle] + [\langle 200 | + \lambda \langle 210 |] \hat{H}_{LI} [|200\rangle + \lambda |210\rangle]) \\ &= \frac{1}{2}(\langle 200 | \hat{H}_{SI} | 200 \rangle + \lambda^2 \langle 210 | \hat{H}_{SI} | 210 \rangle + \lambda \langle 200 | \hat{H}_{SI} | 210 \rangle + \lambda \langle 210 | \hat{H}_{SI} | 200 \rangle \\ &+ \frac{1}{2}(\langle 200 | \hat{H}_{LI} | 200 \rangle + \lambda^2 \langle 210 | \hat{H}_{LI} | 210 \rangle + \lambda \langle 200 | \hat{H}_{LI} | 210 \rangle + \lambda \langle 210 | \hat{H}_{LI} | 200 \rangle) \end{aligned}$$

From here we can make several simplifications. Since $\lambda = \pm 1$, $\lambda^2 = +1$. Regarding the H_{LI} terms, The s orbitals have no orbital angular momentum and so $\langle 200 | \hat{H}_{LI} | 200 \rangle = 0$. Furthermore, since $\vec{B}_L(\vec{0}) \propto \langle \vec{L} \rangle$, $\langle 210 | \hat{H}_{LI} | 210 \rangle = \vec{0}$ because $\langle 210 | \vec{L} | 210 \rangle = 0$. Lastly, the remaining cross terms cancel pairwise and \hat{H}_{LI} contributions nothing to the hyperfine spitting.

$$\begin{aligned} & \langle \phi | \hat{H}_{HF} | \phi \rangle \\ &= \frac{1}{2}(\langle 200 | \hat{H}_{SI} | 200 \rangle + \langle 210 | \hat{H}_{SI} | 210 \rangle + \lambda \langle 200 | \hat{H}_{SI} | 210 \rangle + \lambda \langle 210 | \hat{H}_{SI} | 200 \rangle) \end{aligned}$$

Now we can make some simplifications regarding the \hat{H}_{SI} terms and invoke the previously derived hyperfine structure constants. The first term is between s orbitals, and simplifies to $\langle 200 | \hat{H}_{SI} | 200 \rangle = \frac{2}{3} \frac{E_0(2)}{\hbar^2} \vec{S} \cdot \vec{I} \equiv \frac{\alpha_{200}}{\hbar^2} \vec{S} \cdot \vec{I}$. The second term has been derived in the previous section as well and simplifies to

$$\langle 210 | \hat{H}_{SI} | 210 \rangle = -\frac{E_0(2)}{30} (\vec{S} \cdot \vec{I} - 3\hat{S}_z \hat{I}_z) = -\alpha_{210} (\vec{S} \cdot \vec{I} - 3\hat{S}_z \hat{I}_z). \text{ Finally, the angular}$$

integrals of the two remaining cross terms are both zero. Thus, the expectation value of \hat{H}_{HF} greatly simplifies from the original 8 terms to just two terms:

$$\begin{aligned}
\langle \phi | \hat{H}_{HF} | \phi \rangle &= \frac{1}{2} (\langle 200 | \hat{H}_{SI} | 200 \rangle + \langle 210 | \hat{H}_{SI} | 210 \rangle) \\
&= \frac{1}{2\hbar^2} [(\alpha_{200} - \alpha_{210}) \vec{S} \cdot \vec{I} + 3\alpha_{210} \hat{S}_z \hat{I}_z] \\
&\doteq \frac{1}{2} \begin{pmatrix} \frac{\alpha_{200} + 2\alpha_{210}}{4} & 0 & 0 & 0 \\ 0 & \frac{-\alpha_{200} - 2\alpha_{210}}{4} & \frac{\alpha_{200} - \alpha_{210}}{2} & 0 \\ 0 & \frac{\alpha_{200} - \alpha_{210}}{2} & \frac{-\alpha_{200} - 2\alpha_{210}}{4} & 0 \\ 0 & 0 & 0 & \frac{\alpha_{200} + 2\alpha_{210}}{4} \end{pmatrix}
\end{aligned}$$

This matrix has the same form as the hyperfine matrix in the ground state of hydrogen, and so it is no surprise that it has the same eigenvectors in the $|m_s m_I\rangle$ basis: $|\frac{1}{2}, \frac{1}{2}\rangle$, $|\frac{1}{2}, -\frac{1}{2}\rangle$, $|\Psi^+\rangle$, and $|\Psi^-\rangle$. In the zero-field limit, and in the case of the $|200\rangle$ electronic state, the first three eigenvectors would be the triplet degenerate excited states with $|\Psi^-\rangle$ being the singlet ground state. However, the mixing of $|200\rangle$ with $|210\rangle$ through an external electric field breaks some of this degeneracy as shown in Fig. 1.3. $|\frac{1}{2}, \frac{1}{2}\rangle$ and $|\frac{1}{2}, -\frac{1}{2}\rangle$ remain degenerate but split higher than the triplet energy level, while $|\Psi^+\rangle$ splits lower in energy. In contrast to the hyperfine Stark effect in 1s hydrogen, the emergent splitting of the triplet states is only one order of magnitude smaller than that of the splitting between Ψ^+ and Ψ^- .

These energies and splittings are as follows:

$$\begin{aligned}
E_{|\frac{1}{2}, \frac{1}{2}\rangle} &= E_{|\frac{1}{2}, -\frac{1}{2}\rangle} = \frac{\alpha_{200} + 2\alpha_{210}}{8}, \quad E_+ = \frac{\alpha_{200} - 4\alpha_{210}}{8}, \quad \text{and} \quad E_- = \frac{-3\alpha_{200}}{8} \\
E_{|\frac{1}{2}, \frac{1}{2}\rangle} - E_+ &= \frac{3\alpha_{210}}{4} = 4.93 \text{ neV}, 1.194 \text{ MHz}, \text{ or } 251.3 \text{ meters.} \\
E_+ - E_- &= \frac{\alpha_{200} - \alpha_{210}}{2} = 62.5 \text{ neV}, 1.512 \text{ MHz}, \text{ or } 19.8 \text{ meters.}
\end{aligned}$$

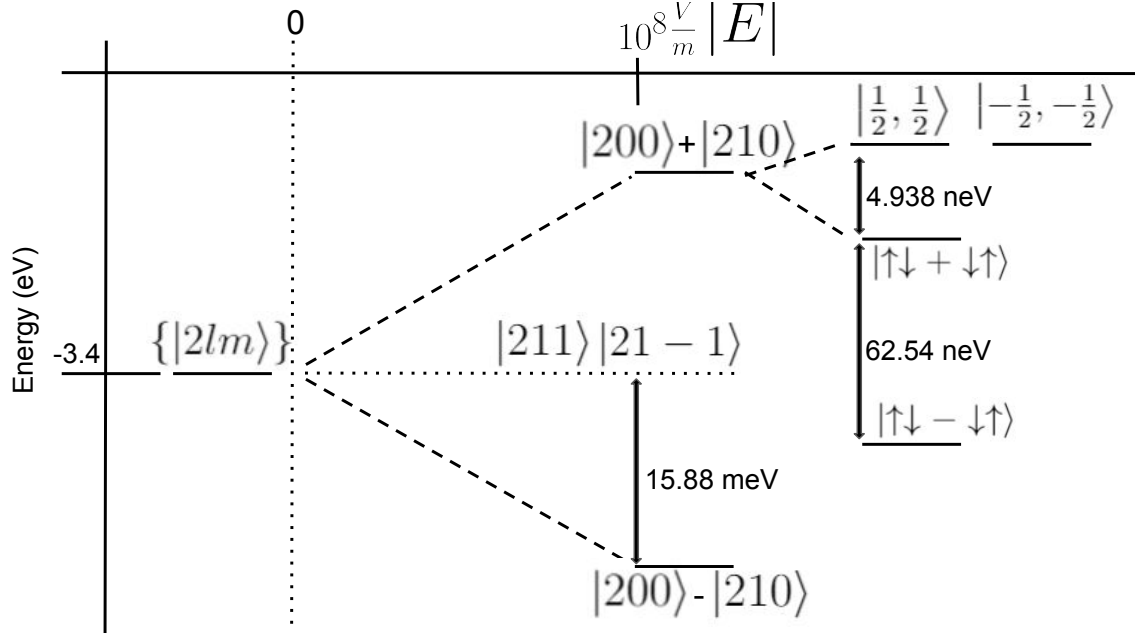


Figure 1.3: Hyperfine Stark effect splitting diagram of Hydrogen 2s

1.11 Combining \hat{H}_{SI} and \hat{H}_{LI} to obtain $\hat{H}_{JI}^{\text{eff}}$

In general we will want to take expectation values of \hat{H}_{HF} , which depends on \vec{S} , \vec{L} , and \vec{I} . It would be convenient if instead of depending on three angular momentum operators, \hat{H}_{HF} only depended on two spin operators, \vec{J} and \vec{I} , where $\vec{J} = \vec{L} + \vec{S}$. In this section, we show that \hat{H}_{SI} and \hat{H}_{LI} can be combined to obtain an effective Hamiltonian in terms of \vec{J} to first order, $\hat{H}_{JI}^{\text{eff}}$. We do this by writing \hat{H}_{HF} in the basis of $|J, m_J, m_I\rangle$ states, fitting the block diagonal elements to $\hat{H}_{JI}^{\text{eff}} = \frac{\chi_J}{\hbar^2} \vec{J} \cdot \vec{I}$, and solving for χ_J .

The first step in this calculation is to use a similarity transformation, using Clebsch-Gordan coefficients, to take \hat{H}_{HF} from the basis of $|L, S, m_l, m_s, m_I\rangle$ to the basis of $|J, m_J, m_I\rangle$. This transformation takes the following form:

$$\hat{H}_{HF|J, m_J, m_I\rangle} \rightarrow \hat{U}^\dagger \hat{H}_{HF|L, S, m_l, m_s, m_I\rangle} \hat{U}$$

Where \hat{U}^\dagger and \hat{U} are unitary matrices with Clebsch-Gordan coefficients as their matrix elements. The columns of \hat{U}^\dagger are the normalized $|L, S, m_l, m_S, m_I\rangle$ states in the basis of the $|J, m_J, m_I\rangle$ states, while the columns of \hat{U} are the normalized $|J, m_J, m_I\rangle$ states in the basis of the $|L, S, m_l, m_S, m_I\rangle$ states. E.g. for $l = 1$, \hat{U}^\dagger is the following 12×12 matrix:

$$\hat{U}^\dagger \doteq \begin{pmatrix} 1 & 0 & 0 & 0 & 0 & 0 & 0 & 0 & 0 & 0 & 0 & 0 & 0 \\ 0 & 1 & 0 & 0 & 0 & 0 & 0 & 0 & 0 & 0 & 0 & 0 & 0 \\ 0 & 0 & \sqrt{\frac{1}{3}} & 0 & \sqrt{\frac{2}{3}} & 0 & 0 & 0 & 0 & 0 & 0 & 0 & 0 \\ 0 & 0 & 0 & \sqrt{\frac{1}{3}} & 0 & \sqrt{\frac{2}{3}} & 0 & 0 & 0 & 0 & 0 & 0 & 0 \\ 0 & 0 & 0 & 0 & 0 & 0 & \sqrt{\frac{2}{3}} & 0 & \sqrt{\frac{1}{3}} & 0 & 0 & 0 & 0 \\ 0 & 0 & 0 & 0 & 0 & 0 & 0 & \sqrt{\frac{2}{3}} & 0 & \sqrt{\frac{1}{3}} & 0 & 0 & 0 \\ 0 & 0 & 0 & 0 & 0 & 0 & 0 & 0 & 0 & 0 & 0 & 1 & 0 \\ 0 & 0 & 0 & 0 & 0 & 0 & 0 & 0 & 0 & 0 & 0 & 0 & 1 \\ 0 & 0 & \sqrt{\frac{2}{3}} & 0 & -\sqrt{\frac{1}{3}} & 0 & 0 & 0 & 0 & 0 & 0 & 0 & 0 \\ 0 & 0 & 0 & \sqrt{\frac{2}{3}} & 0 & -\sqrt{\frac{1}{3}} & 0 & 0 & 0 & 0 & 0 & 0 & 0 \\ 0 & 0 & 0 & 0 & 0 & 0 & \sqrt{\frac{1}{3}} & 0 & -\sqrt{\frac{2}{3}} & 0 & 0 & 0 & 0 \\ 0 & 0 & 0 & 0 & 0 & 0 & 0 & \sqrt{\frac{1}{3}} & 0 & -\sqrt{\frac{2}{3}} & 0 & 0 & 0 \end{pmatrix}$$

However, recall that, in comparison to the bare Hamiltonian, \hat{H}_{Hf} in any angular momentum basis can be treated as a perturbation and so the first-order energy correction is given by the expectation value of \hat{H}_{HF} . Furthermore, in the case of atoms or ions with strong spin-orbit coupling, J and m_J will be good quantum numbers and so the first order energy correction becomes: $\langle J, m_J | \hat{H}_{Hf} | J, m_J \rangle$, which are the diagonal matrix elements in this representation. However, these states are also Kronecker producted to $|m_I\rangle$ states. By including these $|m_I\rangle$ states, the expectation value becomes: $\langle J, m_J, m'_I | \hat{H}_{Hf} | J, m_J, m_I \rangle$, which are the 4×4 block diagonal matrix elements in this representation (for $I = \frac{1}{2}$). Therefore, the matrix we want to use to

find χ_J is \hat{H}_{HF} represented in the $|J, m_J, m_I\rangle$ basis to first order. $\hat{H}_{JI}^{\text{eff}}$ for different values of l and j are tabulated below, using $\beta_{nl} = \frac{E_0(n)}{l(l+1)(2l+1)|g_e|}$:

$$\begin{aligned}
l = 1: \hat{H}_{JI}^{\text{eff}} = & \left. \begin{aligned} -\frac{2}{3\hbar^2} \left(\frac{E_0(n)}{60} - \beta_{n1} \right) \vec{J} \cdot \vec{I} &= \frac{E_0(n)(10-|g_e|)}{90|g_e|\hbar^2} \vec{J} \cdot \vec{I} & j = \frac{3}{2} \\ \frac{4}{3\hbar^2} \left(\frac{E_0(n)}{12} + \beta_{n1} \right) \vec{J} \cdot \vec{I} &= \frac{E_0(n)(2+|g_e|)}{9|g_e|\hbar^2} \vec{J} \cdot \vec{I} & j = \frac{1}{2} \end{aligned} \right| \\
l = 2: \hat{H}_{JI}^{\text{eff}} = & \left. \begin{aligned} -\frac{4}{5\hbar^2} \left(\frac{E_0(n)}{420} - \beta_{n2} \right) \vec{J} \cdot \vec{I} &= \frac{E_0(n)(14-|g_e|)}{525|g_e|\hbar^2} \vec{J} \cdot \vec{I} & j = \frac{5}{2} \\ \frac{2}{5\hbar^2} \left(\frac{E_0(n)}{60} + 3\beta_{n2} \right) \vec{J} \cdot \vec{I} &= \frac{E_0(n)(6+|g_e|)}{150|g_e|\hbar^2} \vec{J} \cdot \vec{I} & j = \frac{3}{2} \end{aligned} \right| \\
l = 3: \hat{H}_{JI}^{\text{eff}} = & \left. \begin{aligned} -\frac{2}{7\hbar^2} \left(\frac{E_0(n)}{504} - 3\beta_{n3} \right) \vec{J} \cdot \vec{I} &= \frac{E_0(n)(18-|g_e|)}{1764|g_e|\hbar^2} \vec{J} \cdot \vec{I} & j = \frac{7}{2} \\ \frac{8}{7\hbar^2} \left(\frac{E_0(n)}{840} + \beta_{n3} \right) \vec{J} \cdot \vec{I} &= \frac{E_0(n)(10+|g_e|)}{735|g_e|\hbar^2} \vec{J} \cdot \vec{I} & j = \frac{5}{2} \end{aligned} \right|
\end{aligned}$$

CHAPTER 2

MULTI-ELECTRON ATOMS

2.1 The Full Many-Body Hamiltonian

For a single-electron system, the energy is described by the kinetic energy of the electron, Coulomb repulsion of the electron and the nucleus, fine structure terms, and hyperfine structure terms. For atoms with many electrons, we can think of adding up many single-electron systems with the addition of interactions between the electrons. Thus, the many-body Hamiltonian takes the following form:

$$\hat{H} = \sum[\hat{H}_0^i + \hat{H}_{fine}^i + \hat{H}_{HF}^i] + \hat{H}_{int}$$

The interactions between electrons are all contained within \hat{H}_{int} and are of several types. However, in this paper we only consider the Coulomb repulsion between electrons and neglect the many other relativistic effects from QED and the Dirac equation. In any case, the electron-electron interactions via electrostatic repulsion only contribute to the total energy and not to the hyperfine splittings.

Since the many-body Hamiltonian is not simply a summation over many single-body Hamiltonians, due to the interaction terms, finding the eigenstates and energies is not a simple matter. Despite this, there are a few rules that can be used to specify the ground state configuration, called Hund's rules.

2.2 Hund's Rules

Hund's rules help us figure out which atomic orbitals will be occupied and with what spin in the ground state configuration, all without having to solve the many-body Schrödinger equation. They do this by taking into account the Pauli exclusion principle, Coulomb repulsion, and spin-orbit coupling.

Hund's first rule has to do with the specification of the total spin $S = |\sum m_s^i|$ of the ground state, and is dictated by the Pauli exclusion principle and Coulomb repulsion. Electrons are fermions, and so the many-body wavefunction must be totally anti-symmetric. Since the wavefunction is a Kronecker product of a spatial part and a spin part there are two options: either the spatial part can be symmetric and the spin part be anti-symmetric, or vice versa. If the spatial part of the many-body wavefunction is symmetric, then the wavefunctions of the individual electrons are allowed to overlap and the electrons will have opposite spins due to the Pauli exclusion principle. Conversely, if we specify that the individual electrons must have the same spin, then by the Pauli exclusion principle their spatial wavefunctions must be anti-symmetric and not overlap. The second option minimizes the Coulomb repulsion because the electrons are on average farther apart, and so we see that the ground state will have as many parallel spins as possible. Thus, Hund's first rule tells us to maximize S first.

Hund's second rule has to do with the specification of the total orbital angular momentum $L = |\sum m_l^i|$ of the ground state, and is dictated by Coulomb repulsion. Thinking classically, each electron orbits the nucleus with some angular momentum. If some electrons orbit the nucleus counterclockwise and other electrons orbit clockwise, at some point the electrons will come very close to each other and there will be a large Coulomb repulsion between them. Conversely, if all of the electrons orbit the

nucleus in the same direction then the average distance between each electron will be maximized, and the Coulomb repulsion between them will be minimized. The second option has lower energy since the Coulomb repulsion will be minimized, and so we see that the ground state will have as many electrons orbiting in the same direction as possible. Furthermore, if the electrons are orbiting in the same direction, then each of their individual orbital angular momenta will have the same sign. Thus, in the quantum picture Hund's second rule tells us to maximize L after maximizing S .

Hund's third rule has to do with the specification of the total angular momentum J of the ground state, and is dictated by spin-orbit coupling. In quantum mechanics the total angular momentum, $\vec{J} = \vec{L} + \vec{S}$, is bounded by the values of L and S : $|L - S| \leq J \leq L + S$. Depending on if the valence shell is greater or less than half full one of these extreme values, $|L - S|$ or $L + S$, will specify the ground state configuration and this specification depends on the spin-orbit coupling. When the shell is less than half full, the total orbital angular momentum will want to align anti-parallel to the total spin angular momentum in order to minimize the spin-orbit energy. Thus, for less than half-filled valence shells, $J = |L - S|$. For more-than-half-filled valence shells this picture becomes tricky. However, it is equivalent to talk about holes with opposite spin, charge, and orbital angular momentum in this limit. If the valence shell is less than half-filled with holes (equivalently more than half-filled with electrons), the total orbital angular momentum will want to align parallel with the total spin angular momentum in order to minimize the spin-orbit energy. Thus, for more-than-half-filled valence shells, $J = L + S$.

2.3 Many-Body Eigenstates and Hyperfine Inner Products

To satisfy Hund's rules, the spatial part of the many-body wavefunction must be totally anti-symmetric in the ground state electronic configuration. To do so, it

is useful to write the wavefunction in terms of a Slater determinant of the single particle wavefunctions. The Slater determinant notation is a compact way of including all possible permutations of the single-particle states while ensuring the totally anti-symmetric condition is satisfied. For example, neutral Carbon has an electron configuration of $[\text{He}]2s^22p^2$ with two valence electrons in the 2p orbitals. By following Hund's rules, we would put one electron in the $\psi_{211}(\vec{r})$ state and the other electron in the $\psi_{210}(\vec{r})$ state. Using a Slater determinant, we could write the many-body wavefunction in the following way:

$$\psi(\vec{r}_1, \vec{r}_2) = \frac{1}{\sqrt{2!}} \begin{vmatrix} \psi_{211}(\vec{r}_1) & \psi_{210}(\vec{r}_1) \\ \psi_{211}(\vec{r}_2) & \psi_{210}(\vec{r}_2) \end{vmatrix} = \frac{1}{\sqrt{2!}} [\psi_{211}(\vec{r}_1)\psi_{210}(\vec{r}_2) - \psi_{211}(\vec{r}_2)\psi_{210}(\vec{r}_1)]$$

However, what we are really interested in is the hyperfine splittings, given by first order perturbation theory, and so we need to know how to generalize the single-electron inner products to the multi-electron picture: $\langle \psi | \hat{H}_{HF} | \psi \rangle = ?$ Luckily, the hyperfine Hamiltonian does not contain any interaction terms and so the many-body hyperfine Hamiltonian is simply a sum over many single-electron hyperfine Hamiltonians: $\langle \psi | \hat{H}_{HF} | \psi \rangle = \langle \psi | \sum \hat{H}_{HF}^i | \psi \rangle$.

$$\begin{aligned} \langle \psi | \hat{H}_{HF} | \psi \rangle &= \frac{1}{2} ({}_1 \langle 211 | {}_2 \langle 210 | - {}_2 \langle 211 | {}_1 \langle 210 |) \hat{H}_{HF} (|211\rangle_1 |210\rangle_2 - |211\rangle_2 |210\rangle_1) \\ &= \frac{1}{2} ({}_1 \langle 211 | {}_2 \langle 210 | - {}_2 \langle 211 | {}_1 \langle 210 |) \sum \hat{H}_{HF}^i (|211\rangle_1 |210\rangle_2 - |211\rangle_2 |210\rangle_1) \end{aligned}$$

Furthermore, since each single-electron Hamiltonian only acts in its own Hilbert space the expectation value simplifies greatly:

$$\begin{aligned} &= \frac{1}{2} ({}_1 \langle 211 | \hat{H}_{SI}^1 + \hat{H}_{LI}^1 |211\rangle_1 + {}_2 \langle 210 | \hat{H}_{SI}^2 + \hat{H}_{LI}^2 |210\rangle_2 + {}_2 \langle 211 | \hat{H}_{SI}^2 + \hat{H}_{LI}^2 |211\rangle_2 \\ &+ {}_1 \langle 210 | \hat{H}_{SI}^1 + \hat{H}_{LI}^1 |210\rangle_1) \\ &= \frac{1}{2} \left[\frac{\alpha_{211}}{\hbar^2} (\vec{S}^1 \cdot \vec{I} - 3\hat{S}_z^1 \hat{I}_z) + \frac{\beta_{211}}{\hbar^2} \vec{L}^1 \cdot \vec{I} - \frac{|\alpha_{210}|}{\hbar^2} (\vec{S}^2 \cdot \vec{I} - 3\hat{S}_z^2 \hat{I}_z) + \frac{\beta_{210}}{\hbar^2} \vec{L}^2 \cdot \vec{I} \right. \\ &+ \left. \frac{\alpha_{211}}{\hbar^2} (\vec{S}^2 \cdot \vec{I} - 3\hat{S}_z^2 \hat{I}_z) + \frac{\beta_{211}}{\hbar^2} \vec{L}^2 \cdot \vec{I} - \frac{|\alpha_{210}|}{\hbar^2} (\vec{S}^1 \cdot \vec{I} - 3\hat{S}_z^1 \hat{I}_z) + \frac{\beta_{210}}{\hbar^2} \vec{L}^1 \cdot \vec{I} \right] \end{aligned}$$

However, recall that $\beta_{21m} \propto \vec{B}_L(\vec{0}) \propto m_l$, so $\beta_{210} = 0$. We can further simplify the expression by combining terms of alike quantum hyperfine structure constants:

$$= \frac{1}{2} \left[\frac{\alpha_{211}}{\hbar^2} ([\vec{S}^1 + \vec{S}^2] \cdot \vec{I} - 3[\hat{S}_z^1 + \hat{S}_z^2] \hat{I}_z) - \frac{|\alpha_{210}|}{\hbar^2} ([\vec{S}^1 + \vec{S}^2] \cdot \vec{I} - 3[\hat{S}_z^1 + \hat{S}_z^2] \hat{I}_z) + \frac{\beta_{211}}{\hbar^2} [\vec{L}^1 + \vec{L}^2] \cdot \vec{I} \right]$$

Next, we can write the single-electron angular momentum operators in terms of the many-body total angular momentum operators, $\vec{S}^1 + \vec{S}^2 = \vec{S}$, $\hat{S}_z^1 + \hat{S}_z^2 = \hat{S}_z$ and $\vec{L}^1 + \vec{L}^2 = \vec{L}$, which simplifies our expression even further:

$$\begin{aligned} &= \frac{1}{2} \left[\frac{\alpha_{211}}{\hbar^2} (\vec{S} \cdot \vec{I} - 3\hat{S}_z \hat{I}_z) - \frac{|\alpha_{210}|}{\hbar^2} (\vec{S} \cdot \vec{I} - 3\hat{S}_z \hat{I}_z) + \frac{\beta_{211}}{\hbar^2} \vec{L} \cdot \vec{I} \right] \\ &= \frac{\alpha_{avg}}{\hbar^2} (\vec{S} \cdot \vec{I} - 3\hat{S}_z \hat{I}_z) + \frac{\beta_{avg}}{\hbar^2} \vec{L} \cdot \vec{I} \end{aligned}$$

Where, by using Hund's rules, we know that total $S = 1$ and total $L = 1$. We can generalize this result to any number of particles in the $|m_l, m_s, m_I\rangle$ basis. If we use a Slater determinant to express every possible permutation of single-particle states, the many-body hyperfine structure constants end up being simply the average value of the possible single-particle hyperfine structure constants. Then to determine the value of total S and total L, we need only remember Hund's first two rules.

2.4 Many-Body Spin Operators

Generally speaking, it will be useful to know how to sum several single electron angular momentum operators, weighted by different hyperfine structure constants, in terms of the total angular momentum operator. For example, consider a three-particle system where $\vec{S}^1 + \vec{S}^2 + \vec{S}^3 = \vec{S}$. Suppose throughout the course of determining the hyperfine splitting we obtain the following expression, which we let equal some unknown \hat{F} for clarity: $\alpha_i \vec{S}^1 + \alpha_j \vec{S}^2 + \alpha_k \vec{S}^3 = \hat{F}(\vec{S})$, where I have omitted the usual factors of \hbar for simplicity.

The previous equation does not immediately seem to simplify to an expression

containing \vec{S} , but we can make that happen by invoking the indistinguishable nature of electrons. There is nothing that distinguishes electron 1 from electron 2 or 3, and so if we write down all possible permutations of our equation, they must all equal $\hat{F}(\vec{S})$. Therefore, if we add up all six possible permutations of the electron indices, this new equation still must equal $\hat{F}(\vec{S})$. Using this trick we obtain:

$$\begin{aligned}
6\hat{F}(\vec{S}) &= \alpha_i\vec{S}^1 + \alpha_j\vec{S}^2 + \alpha_k\vec{S}^3 + \alpha_i\vec{S}^1 + \alpha_j\vec{S}^3 + \alpha_k\vec{S}^2 + \alpha_i\vec{S}^2 + \alpha_j\vec{S}^1 + \alpha_k\vec{S}^3 \\
&+ \alpha_i\vec{S}^2 + \alpha_j\vec{S}^3 + \alpha_k\vec{S}^1 + \alpha_i\vec{S}^3 + \alpha_j\vec{S}^1 + \alpha_k\vec{S}^2 + \alpha_i\vec{S}^3 + \alpha_j\vec{S}^2 + \alpha_k\vec{S}^1
\end{aligned}$$

By collecting the terms with the same hyperfine structure constants we obtain:

$$\begin{aligned}
6\hat{F}(\vec{S}) &= 2\alpha_i[\vec{S}^1 + \vec{S}^2 + \vec{S}^3] + 2\alpha_j[\vec{S}^1 + \vec{S}^2 + \vec{S}^3] + 2\alpha_k[\vec{S}^1 + \vec{S}^2 + \vec{S}^3] \\
&= 2\alpha_i\vec{S} + 2\alpha_j\vec{S} + 2\alpha_k\vec{S} = 2(\alpha_i + \alpha_j + \alpha_k)\vec{S}
\end{aligned}$$

And we see $\alpha_i\vec{S}^1 + \alpha_j\vec{S}^2 + \alpha_k\vec{S}^3 = \hat{F}(\vec{S}) = \alpha_{avg}\vec{S}$. Thus, if we have a sum of N single-electron angular momentum operators weighted by different hyperfine structure constants, to write this in terms of the total angular momentum operator we need only average the single-electron hyperfine structure constants.

CHAPTER 3

TRIPLY IONIZED TERBIUM

3.1 Electronic Configuration and Ground State

Terbium has atomic number 65 and is one of the lanthanides, with ^{159}Tb being its only stable isotope. Neutral terbium has the electronic configuration $[\text{Xe}]4f^96s^2$, and exhibits paramagnetism because of the unpaired f electrons. When terbium bonds it acts an electron donor, and in the case of TbPc_2 it donates three electrons. Thus, Tb^{3+} has the electronic configuration of $[\text{Xe}]4f^8$, and is more paramagnetic than neutral terbium due to a greater number of unpaired electrons. In this section, we model Tb^{3+} as an atom with 8 $4f$ electrons with an effective Clementi-Raimondi⁸ nuclear charge, $Z_{\text{eff}} = 25.865$, to account for the atomic shielding. We also use the nuclear g -factor, $g_N = 1.354$, from Ref. 1 and Ref. 9.

To find the ground-state configuration of terbium we need only apply Hund's rules, rather than solve the many-body Schrödinger equation. We have an unfilled $4f$ shell, $l = 3$ and $-3 \leq m_l \leq 3$, which can hold up to 14 electrons and we need to know how to arrange 8 electrons in it. Following Hund's first rule, we first maximize S . There are 7 orbitals which can each hold 2 electrons of different spin and so to maximize S we put 2 electrons of different spin in one orbital, while putting one up-spin electron in each of the remaining orbitals. The spins of electrons in the filled orbital cancel, and the other 6 up-spin electrons sum to give $S = 3$.

We use Hund's second rule to determine which orbital to put the down-spin

electron, which tells us to maximize L . First we realize that the orbital angular momentum of each of the up-spin electrons cancel pairwise (except for the $m_l = 0$ state which has no orbital angular momentum), and so it is only the down-spin electron which will carry angular momentum. Thus, we give this electron the largest amount of angular momentum possible, $m_l = 3$, and we see that $L = 3$. We summarize this configuration in the following table:

| | | | | | | |
|------------|------------|------------|-----------|-----------|-----------|-----------|
| $m_l = -3$ | $m_l = -2$ | $m_l = -1$ | $m_l = 0$ | $m_l = 1$ | $m_l = 2$ | $m_l = 3$ |
| ↑ | ↑ | ↑ | ↑ | ↑ | ↑ | ↑↓ |

Finally, we will want to know what the ground state is in the $|J, m_J\rangle$ basis and so we use Hund's third rule. For a more than half-filled shell, $J = L + S$, and so we see $J = 6$ due to spin-orbit coupling effects.

3.2 The Effective 6-Particle State

In this section we argue that for the purpose of calculating hyperfine splittings, it is sufficient to use a configuration of six electrons instead of eight. Consider two electrons with opposite spin and orbital angular momentum. Recall the previously derived formula for the magnetic field at the nucleus due to the orbital motion of the electrons:

$$\vec{B}_L(\vec{0}) = -\frac{m_l \mu_0 \mu_B Z_{\text{eff}}^3}{\pi n^3 a_0^3 l(l+1)(2l+1)} \hat{e}_z$$

Thus, we see that for two states of orbital angular momentum quantum numbers m_l and $-m_l$, these two magnetic fields cancel pairwise at the origin as do their contributions to the hyperfine splitting through \hat{H}_{LI} .

Furthermore, if the spins of these electrons are opposite, \vec{S}^i and $-\vec{S}^j$, we could equivalently say that their hyperfine structure constants are of opposite signs and their spins are the same. Thus, when we sum the single electron spins and their

hyperfine structure constants to get $\alpha_{avg}\vec{S}$, their effects will cancel pairwise in H_{SI} as well.

The two electrons in question are the down-spin electron in the $|433\rangle$ state and the up-spin electron in the $|43-3\rangle$ state. If we accept that removing two electrons of opposite spin and orbital angular momentum from the electron configuration doesn't destroy any information, our lives become much easier in the coming sections. If we make this simplification and use this particular effective 6-particle state, S and L still remain invariant and the many-body wavefunction has less permutations to account for. The only caveat is that the 6-particle state should technically have $J = 0$, since the shell is less than half-filled. However, this 6-particle state does not have physical meaning and is only a mathematical tool. Thus, we will just have to remember that since the physically meaningful 8-particle state had $J = 6$, so too must the effective, non-physical 6-particle state. We succinctly summarize this effective configuration in the following table:

| | | | | | | |
|------------|------------|------------|-----------|-----------|-----------|-----------|
| $m_l = -3$ | $m_l = -2$ | $m_l = -1$ | $m_l = 0$ | $m_l = 1$ | $m_l = 2$ | $m_l = 3$ |
| | ↑ | ↑ | ↑ | ↑ | ↑ | ↑ |

3.3 LS vs. jj Coupling

Terbium is a heavy element with considerable spin-orbit coupling. The formula for the orbital speed given by the Bohr theory¹⁰, $v = \frac{Z_{\text{eff}}e^2}{4\pi\epsilon_0 n\hbar}$, gives an estimate of $v = 0.047c$ for terbium. While this estimate for the orbital speed may not seem very significant, it's over 6 times that of Hydrogen.

The many-body hyperfine Hamiltonian is luckily just a sum over the single-body hyperfine Hamiltonians, but the crux of the issue comes when trying to form a many-body $\hat{H}_{JJ}^{\text{eff}}$. There are two options: sum up the single-body hyperfine Hamiltonians in the $|M_l M_S\rangle$ basis and then match it to an effective $\hat{H}_{JI}^{\text{eff}}$ to first order, or match

all of the single-body Hamiltonians to effective single body $\hat{H}_{JI}^{\text{eff}}$ and then sum those up. The first option is called LS coupling and the second option is called jj coupling. We use LS coupling when the spin-orbit interaction is weak, and jj coupling when the spin-orbit interaction is strong.

It turns out that light atoms like carbon (atomic number 6) are well-described by LS coupling, while heavy elements like lead (atomic number 82) are well-described by jj coupling. Terbium (atomic number 65) is not a light element, nor as heavy as lead, and so it is likely that neither LS nor jj coupling is completely accurate. In the following sections we will calculate hyperfine splittings in both schemes to glean an estimated range of the true hyperfine splittings.

3.4 Hyperfine Splittings in the LS Coupling Scheme

In the LS coupling scheme, we start by forming the many-body \hat{H}_{HF} in the $|M_L, M_S, m_I\rangle$ basis. Since $\hat{H}_{HF} = \sum \hat{H}_{HF}^i$, we need only sum up the single-electron Hamiltonians of the effective 6-particle state to get a many-body Hamiltonian in terms of total S and L. We will also want to eventually go to the $|J, M_J, m_I\rangle$ basis so we should use $\hat{H}_{SI}^{\text{eff}}$ for $l = 3$, instead of \hat{H}_{SI} and evaluating the hyperfine structure constants outright. It turns out that the many-body $\hat{H}_{SI}^{\text{eff}}$ takes the following form:

$$\begin{aligned}\hat{H}_{SI}^{\text{eff}} &= \sum \hat{H}_{SI}^{\text{eff},i} = \sum \frac{1}{168} \frac{E_0(n)}{\hbar^2} \left(\frac{8}{15} \vec{S}^i \cdot \vec{I} - \frac{2}{15} \frac{(\vec{L} \cdot \vec{I})(\vec{L} \cdot \vec{S}^i) + (\vec{L} \cdot \vec{S}^i)(\vec{L} \cdot \vec{I})}{2} \right) \\ &= \frac{1}{168} \frac{E_0(n)}{\hbar^2} \left(\frac{8}{15} \vec{S} \cdot \vec{I} - \frac{2}{15} \frac{(\vec{L} \cdot \vec{I})(\vec{L} \cdot \vec{S}) + (\vec{L} \cdot \vec{S})(\vec{L} \cdot \vec{I})}{2} \right)\end{aligned}$$

Where Hund's rules tell us that the ground state should have total $L = 3$ and total $S = 3$. To obtain the above expression, we made the simplification that $\vec{L}^i \equiv \vec{L}$ and $l^i = L = 3$ since it is only the orbital angular momentum of the up-spin $|433\rangle$ electron that contributes to total L. We also write down the many-body \hat{H}_{LI} :

$$\hat{H}_{LI} = \sum \hat{H}_{LI}^i = \sum \frac{\beta^i}{\hbar^2} \vec{L}^i \cdot \vec{I}$$

As stated above, the orbital angular momenta of all but the $|433\rangle$ electron either cancel pairwise or are zero and we can let $\vec{L}^{433} \equiv \vec{L}$. Thus, the many-body \hat{H}_{LI} can be written only in terms of the $|433\rangle$ electron and we obtain an expression for the many-body $\hat{H}_{HF}^{\text{eff}}$:

$$\hat{H}_{LI} = \frac{\beta_{43}}{\hbar^2} \vec{L} \cdot \vec{I}, \text{ and } \hat{H}_{HF}^{\text{eff}} = \frac{1}{168} \frac{E_0(n)}{\hbar^2} \left(\frac{8}{15} \vec{S} \cdot \vec{I} - \frac{2}{15} \frac{(\vec{L} \cdot \vec{I})(\vec{L} \cdot \vec{S}) + (\vec{L} \cdot \vec{S})(\vec{L} \cdot \vec{I})}{2} \right) + \frac{\beta_{43}}{\hbar^2} \vec{L} \cdot \vec{I}$$

After following the same procedure as in section 1.11, we obtain an effective first-order $\hat{H}_{JI}^{\text{eff}}$ for $J = 6$, describing the manifold of ground states according to Hund's rules:

$$\hat{H}_{JI}^{\text{eff}} = \frac{1}{2\hbar^2} \left(-\frac{E_0(n)}{252} + \beta_{43} \right) \vec{J} \cdot \vec{I} = \frac{E_0(n)}{504|g_e|\hbar^2} (3 - |g_e|) \vec{J} \cdot \vec{I} \equiv \frac{\chi_J}{\hbar^2} \vec{J} \cdot \vec{I}$$

According to Ref. 2, the phthalocyanine ligands in TbPc₂ have the effect of creating an easy-axis anisotropic energy level manifold among the $|J = 6, M_J\rangle$ states, as shown in Fig. 3.1. As we see in Figs. 4.2 and 4.3, the ligands contribute a large amount of electric charge in planar distributions above and below the terbium atom and in order to minimize the Coulomb repulsion, terbium's electrons will prefer to be in a planar distribution. This means that $m_l = \pm 3$ states are preferred, maximizing the amount of total \vec{L} along the z-axis. Furthermore, the spin-orbit energy is minimized when total \vec{S} is parallel to total \vec{L} , which maximizes the amount of total \vec{S} along the z-axis. All effects considered, the z-axis becomes an easy axis of magnetization. Thus, the states of equal $|M_J|$ are degenerate and the $|J = 6, M_J = \pm 6\rangle$ form a ground-state doublet. Furthermore, the states $|M_J\rangle = \pm 6$ and $|M_J\rangle = \pm 5$ are separated² by approximately 600 Kelvin. Thus, when calculating hyperfine splittings, we may fix $J = M_J = 6$ and calculate splittings between adjacent $|M_J, m_I\rangle$ and $|M_J, m'_I\rangle$ states, instead of going to the combined angular momentum basis as we did in sections 1.8, 1.9, and 1.10:

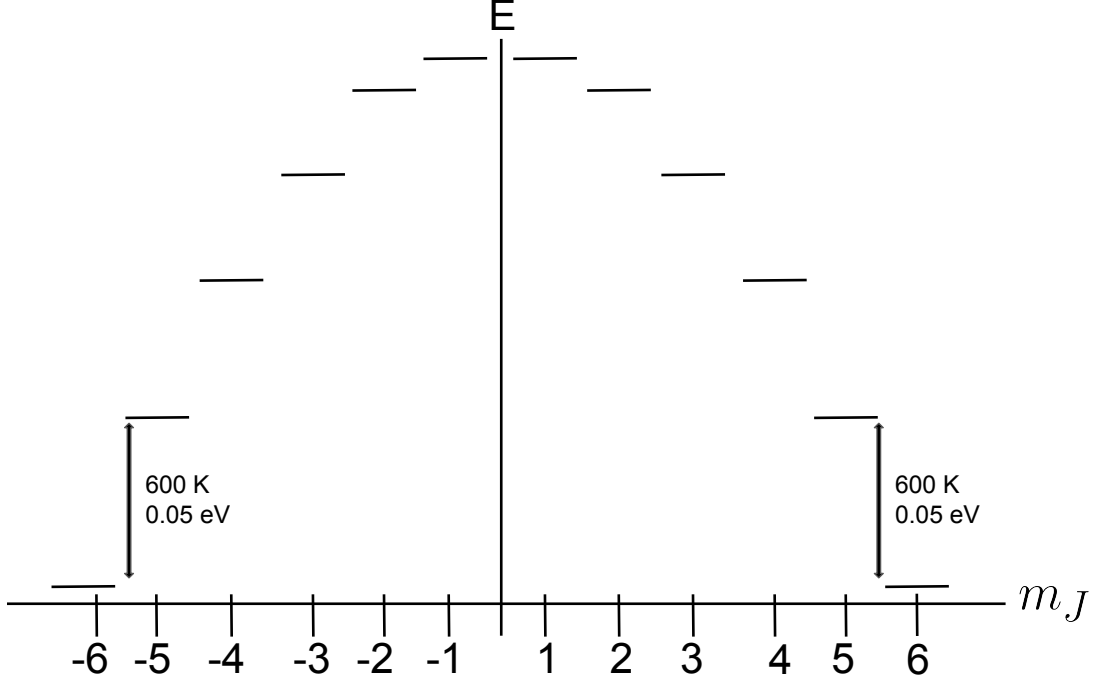


Figure 3.1: Approximate energy level diagram of the $|J = 6, M_J\rangle$ states of Tb^{3+} due to the phthalocyanine ligands

$$\begin{aligned} \Delta E_{HF} &= \langle 6, m'_I | \hat{H}_{JI}^{\text{eff}} | 6, m'_I \rangle - \langle 6, m_I | \hat{H}_{JI}^{\text{eff}} | 6, m_I \rangle \\ &= 6\chi_J \Delta m_I = 6\chi_J = 3.44 \mu\text{eV}, \end{aligned}$$

which corresponds to a frequency of 2.75 GHz. These splittings agree closely with Ref. 1, on the order of a few GHz. However, in the above calculation we deduced the effective coupling parameter, χ_J , by calculating the energy of “classical” states of maximum spin and comparing this result to the effective quantum Hamiltonian. In our future work we aim to reconcile this classical approach with fully quantum mechanical calculations.

3.5 Hyperfine Splittings in the jj Coupling Scheme

In the jj coupling scheme, we simply need to add up the correct single electron effective Hamiltonians, $\hat{H}_{JI}^{\text{eff},i}$, from section 1.11 and use the previously derived relation:

$$\sum \frac{\chi_i}{\hbar^2} \vec{J}^i \cdot \vec{I} = \frac{\chi_{avg}}{\hbar^2} \vec{J} \cdot \vec{I} \equiv \hat{H}_{JI}^{eff}$$

However, Hund's rules only describe the ground state configuration in the LS scheme, and so we need a different set of rules in the jj scheme. Each electron has $s = \frac{1}{2}$ and $l = 3$, so the total angular momentum of each electron can be $j = \frac{7}{2}$ or $\frac{5}{2}$. This makes it difficult to describe the total angular momentum, $\vec{J} = \sum \vec{J}^i$, and to know which $\hat{H}_{JI}^{eff,i}$ to sum. According to Ref. 11, the $j = l - \frac{1}{2}$ manifold has lowest energy and so we fill those states first, starting with the states with the highest value of m_j in order to maximize total $J = |\sum m_j|$. Then we fill the $j = l + \frac{1}{2}$ manifold, if necessary, in the same way. These rules tell us that 6 of terbium's 4f electrons have $j = \frac{5}{2}$, 2 have $j = \frac{7}{2}$, and total $J = 6$. This is summarized in the term symbol, $[(f_{\frac{5}{2}})^6(f_{\frac{7}{2}})^2]_6$. Furthermore, it is good to know that at the end of the day the jj and LS schemes agree on the value of the total J, regardless of the route to get there.

Since all of the $j = \frac{5}{2}$ states are occupied, this manifold has zero net angular momentum and therefore it does not contribute to the hyperfine splittings. Thus, the only electrons that contribute to the hyperfine splittings are the two $j = \frac{7}{2}$ electrons, which have $m_j = \frac{7}{2}$ and $\frac{5}{2}$. We can use this information to write down \hat{H}_{JI}^{eff} by simply calculating χ_{avg} :

$$\chi_{avg} = \frac{1}{2}[2\chi_{\frac{7}{2}}] = \chi_{\frac{7}{2}} = \frac{E_0(n)(18-|g_e|)}{1764|g_e|}$$

Now that we have \hat{H}_{JI}^{eff} , we can apply the same logic as in the case of LS coupling to calculate the splittings between adjacent $|M_J, m_I\rangle$ and $|M_J, m'_I\rangle$ states:

$$\Delta E_{HF} = \langle 6, m'_I | \hat{H}_{JI}^{eff} | 6, m'_I \rangle - \langle 6, m_I | \hat{H}_{JI}^{eff} | 6, m_I \rangle$$

$$= 6\chi_J \Delta m_I = 6\chi_J = 16.6 \mu\text{eV}, \text{ which corresponds to a frequency of 4.01 GHz.}$$

This result also agrees closely with the results of Ref. 1, on the order of a few GHz. As in the previous section, in the above calculation we deduced the effective coupling parameter, χ_J , by calculating the energy of "classical" states of maximum spin and

comparing this result to the effective quantum Hamiltonian. In our future work we aim to reconcile this classical approach with fully quantum mechanical calculations.

Thus, our calculations estimate the hyperfine splitting between adjacent $|m_I\rangle$ states is bounded between $2.75 \text{ GHz} \leq f_{\text{true}} \leq 4.01 \text{ GHz}$.

3.6 The Hyperfine Stark Effect

If we take an individual electron in a 4f orbital and place it in an electric field along the z axis, we can use first-order time-independent perturbation theory to estimate the form of the new wavefunction (as in Sec. 1.9). We can then generalize this result to the case of several 4f electrons, as in Tb^{3+} , and attempt to follow the same course of action as Section 3.3.

The selection rules of the Stark Effect state that matrix elements of $-\vec{p} \cdot \vec{E} = e|E|\hat{z}$ only survive for $\Delta l = \pm 1$ and $\Delta m = 0$. Thus, for a 4f electron in state $|43m\rangle$ it can only couple to states $|n, l \pm 1, m\rangle$, such as the 5d and 5g states. Using first order perturbation theory and keeping only the largest terms in the infinite sum, we obtain an expression for the first order corrected wavefunction:

$$|\phi_p\rangle = |43m\rangle + \gamma_m |52m\rangle + \delta_m |54m\rangle$$

Using the effective 6-particle state, we tabulate the single-body corrected wavefunctions here:

$$|\phi_p^3\rangle = |433\rangle + \delta_3 |543\rangle$$

$$|\phi_p^2\rangle = |432\rangle + \gamma_2 |522\rangle + \delta_2 |542\rangle$$

$$|\phi_p^1\rangle = |431\rangle + \gamma_1 |521\rangle + \delta_1 |541\rangle$$

$$|\phi_p^0\rangle = |430\rangle + \gamma_0 |520\rangle + \delta_0 |540\rangle$$

$$|\phi_p^{-1}\rangle = |43-1\rangle + \gamma_{-1} |52-1\rangle + \delta_{-1} |54-1\rangle$$

$$|\phi_p^{-2}\rangle = |43 - 2\rangle + \gamma_{-2} |52 - 2\rangle + \delta_{-2} |54 - 2\rangle$$

Since all of the first order corrected states are orthogonal, we can use the results of sections 1.9, 2.3, and 3.4 to obtain the following many-body hyperfine Hamiltonian in the LS coupling scheme:

$$\hat{H}_{HF} = [\hat{H}_{SI}^{\text{eff}} + \hat{H}_{LI}]_{4f} + \gamma_{avg}^2 [\hat{H}_{SI}^{\text{eff}} + \hat{H}_{LI}]_{5d} + \delta_{avg}^2 [\hat{H}_{SI}^{\text{eff}} + \hat{H}_{LI}]_{5g}$$

However, it turns out that $\gamma_m \sim 10^{-49}|E|$ and $\delta_m \sim 10^{-48}|E|$. Therefore, when it comes to forming this many-body Hamiltonian, the two new terms due to the coupling with the 5d and 5g states $\sim 10^{-98}|E|^2$ or $\sim 10^{-96}|E|^2$ respectively, and are negligible even for the most extreme electric fields. Thus, the hyperfine Stark effect is a moot point in triple-ionized terbium due to the extremely weak coupling of adjacent l states through the electric field.

CHAPTER 4

THE HYPERFINE STARK EFFECT IN TBPC₂

4.1 Introduction to Density Functional Theory

As we saw in the previous chapter, the complexity of the calculation increases tremendously with the number of atoms. This is because we need to keep track of 3 spatial degrees of freedom for every electron. In addition, to impose the condition that the electrons are indistinguishable we need to use a Slater determinant, which grows in size as $N!$. Furthermore, if there is more than one atom, then we need to keep track of the spatial degrees of freedom of the nuclei as well. Thus, for N electrons and M nuclei, we have $3(N + M)$ spatial degrees of freedom alone! We also need to account for the electronic and nuclear spin degrees of freedom. At a certain point, the complexity of molecular calculations scale beyond the power of traditional quantum mechanics, even with the most advanced computing power.

Density functional theory (DFT) relies on a theorem which states that the total energy of the ground state is a functional of the electron density. Therefore, instead of minimizing the energy with respect to a $3N$ -dimensional wavefunction, we can minimize the energy with respect to a 3-dimensional electron density. This greatly reduces the computational complexity of the problem. However, the true form of the energy functional is unknown, and so DFT does not give exact results. Nonetheless, good approximations to the energy functional do exist, and when used correctly DFT can produce very accurate approximations that agree closely with experiments.

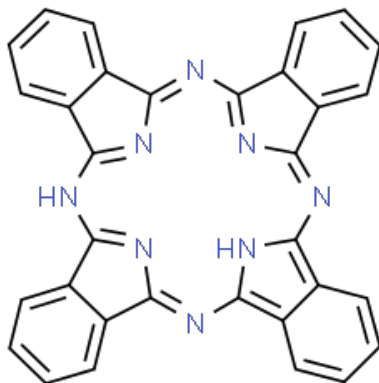


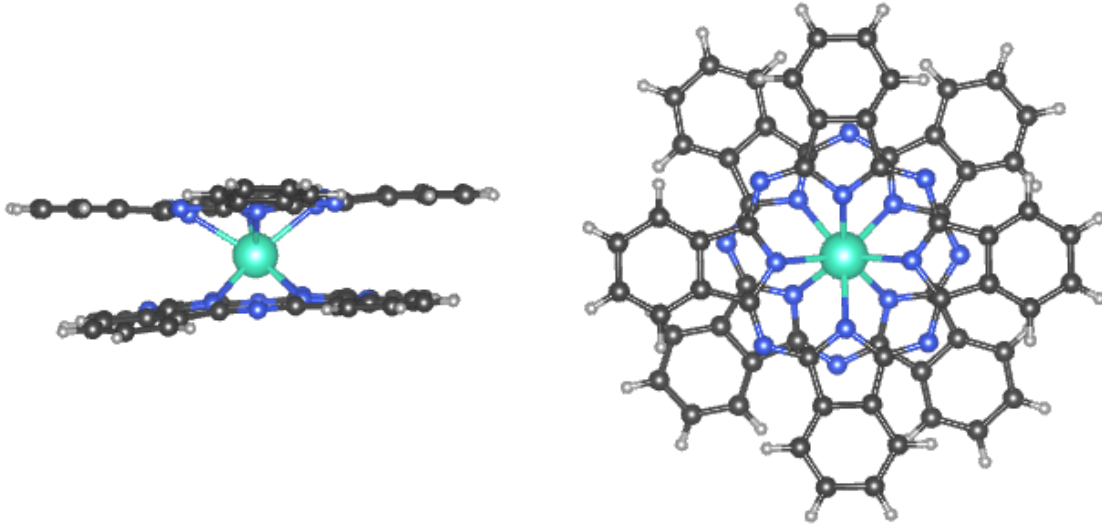
Figure 4.1: Structural diagram of one phthalocyanine ligand.

4.2 TbPc₂

Bisphthalocyaninato terbium(III), TbPc₂, is a metal-organic compound consisting of a terbium atom sandwiched between two 2D phthalocyanine organic ligand structures. Through the bonding process, terbium donates three electrons to the ligands and becomes triple-ionized. We show a structural diagram of one phthalocyanine molecule in Fig. 4.1, from which TbPc₂ is derived. In TbPc₂, the terbium ion is 8-fold coordinated to the Nitrogen atoms in the ligands, which are located nearest to the center of the molecule. The molecule also acts as a single molecule magnet, whose magnetic properties can be tailored by altering the structure and/or composition of the ligands. A rendering of this molecule in VESTA software is shown in Fig. 4.2a and Fig. 4.2b.

4.3 VASP Calculations

The first step in calculating the hyperfine Stark effect in TbPc₂ is to determine the electronic structure of the molecule using DFT. In this section, we present an attempt at this using the Vienna Ab initio Simulation Package (VASP) with appropriate



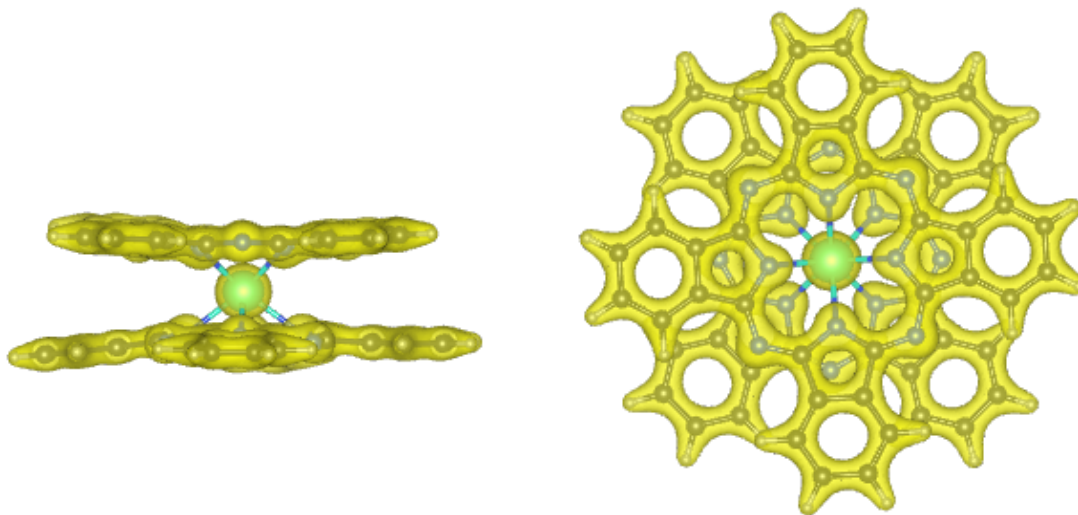
(a) Side view of TbPc_2 . The turquoise atom in the center is the Tb^{3+} ion, which is 8-fold coordinated to the nitrogen atoms (blue) of the two phthalocyanine ligands. We see that each ligand is approximately planar.

(b) Top view of TbPc_2 . We see the phthalocyanine ligands are rotated approximately 45 degrees with respect to each other.

Figure 4.2: Rendering of TbPc_2 in VESTA

parameters.

We used the VASP code to relax the positions of the atoms in order to obtain a rough idea of the electronic structure of the molecule. Although DFT is generally not extremely accurate for the well-localized f orbitals we are mainly using VASP to calculate the ligand field, which DFT works well for. We form a simple cubic lattice of TbPc_2 , but with a large lattice parameter of 30 \AA to minimize intermolecular interactions. We used the Perdew, Burke, and Ernzerhof (PBE) exchange correlation functional, and set the plane wave cutoff $\text{ENMAX} = 240 \text{ eV}$ for a coarse-grained proof-of-principle calculation. Of course if one was to accurately calculate the ligand field using VASP, it would be advisable to set $\text{ENMAX} = 400 \text{ eV}$ for a more accurate result. To treat the $4f$ electrons, we used a Hubbard correction term $\text{LDAUU} = 5 \text{ eV}$, and an exchange parameter $\text{LDAUJ} = 0.7 \text{ eV}$ using Ref. 12 as a guide. A rendering of the CHGCAR file in VESTA is shown in Fig. 4.3a and Fig. 4.3b, setting the



(a) Side view of TbPc_2 at a particular surface of constant electric charge density. (b) Top view of TbPc_2 at a particular surface of constant electric charge density.

Figure 4.3: Rendering of the CHGCAR file in VESTA

isosurface parameter to 0.15. For this calculation, we simulated an isolated neutral TbPc_2 molecule, whereas the electronic structure of $[\text{TbPc}_2]^-$ may differ somewhat.

CHAPTER 5

CONCLUSIONS AND FUTURE WORK

5.1 Conclusions

By the end of chapter 1, we were able to calculate the hyperfine Stark effect of any single-electron system and demonstrated this for hydrogen 1s and 2s. We started by calculating the hyperfine splitting in hydrogen 1s to show that our calculations reproduce the famous 21 cm line. We then used first-order time-independent perturbation theory to calculate the effect of an external electric field on the wavefunctions of hydrogen 1s and 2s. Using the perturbed wavefunctions we calculated the hyperfine splittings, ignoring fine structure effects.

In chapter 3 we showed that the hyperfine Stark effect in an isolated Tb^{3+} ion is a negligible effect. To do this, we first used the derivations for many-body electronic states and angular momenta operators from chapter 2 to calculate the hyperfine splittings. Modeling the manifold of ground M_J states as they would be under the easy axis anisotropic effect of the phthalocyanine ligands, we used the LS and jj coupling schemes to calculate a range of hyperfine splittings of adjacent m_I states, $2.75 \text{ GHz} \leq f_{\text{true}} \leq 4.01 \text{ GHz}$. This range of splittings agrees with Ref. 1, which states that the hyperfine splittings of TbPc_2 should be on the order of a few GHz in the zero-field regime. Finally, we used first-order time-independent perturbation theory to calculate the perturbation of the many-body wavefunction due to an external electric field. In doing so, we showed that the additional terms in the Hamiltonian

due to the coupling of the 4f states with the 5d and 5g states $\sim 10^{48}$ or $\sim 10^{-49}$, rendering the hyperfine Stark effect negligible.

However, this is not the end of the story. Although the hyperfine structure constants of Tb^{3+} cannot be substantially modulated by electric fields, we do not expect the same to hold true for TbPc_2 as explained in the next section.

5.2 Future Work

In this section we present a road-map for calculating the hyperfine Stark effect in TbPc_2 , and how one might enhance it, starting from where we left off in chapter 4. This entails treating the electronic charge density of the ligands as an external potential in which triply ionized terbium's 4f electrons sit, perturbing the many-body wavefunction. Furthermore, we expect that placing this entire structure in an electric field will have a much greater effect on the hyperfine splittings than the negligible effect we calculated in section 3.6, due to the presence of the ligand field.

After the VASP calculations are complete one obtains, among other things, the numerically-determined electrostatic charge density of the ligands. In order to use the framework developed in chapters 1-3, it makes sense to expand the ligand field in the basis of spherical harmonics. We may use the interior spherical multipole expansion to do this¹³:

$$V_{ligand}(\vec{r}) = \frac{1}{4\pi\epsilon_0} \sum B_{lm} r^l Y_{lm}(\theta, \phi)^*, \text{ where } B_{lm} = \frac{4\pi}{2l+1} \int \frac{1}{r^{l+1}} Y_{lm}(\theta, \phi) \rho_{ligand}(\vec{r}) d^3r$$

From here we use first-order perturbation theory. If we let $|\psi_{4f8}\rangle$ be the many-body wavefunction of Tb^{3+} , then the first-order correction to this wavefunction, denoted $|\psi'\rangle$ becomes:

$$|\psi'\rangle = |\psi_{4f8}\rangle + \sum \frac{\langle \phi_i | V_{ligand} | \psi_{4f8} \rangle}{E_{4f8} - E_i} |\phi_i\rangle,$$

where the states $|\phi_i\rangle$ are likely to be the 5d states with the opposite parity of the $|\psi_{4f8}\rangle$ states, due to TbPc₂ lacking inversion symmetry. Since the $|\psi_{4f8}\rangle$ states are orthogonal to the $|\phi_i\rangle$, one can use the same procedures as in sections 3.4, 3.5, and 3.6 to calculate the hyperfine splittings in the zero-field regime.

Once we switch on an electric field the wavefunction becomes further perturbed. Letting $|\psi''\rangle$ be the first-order correction to previously perturbed many-body wavefunction, we obtain an expression for the wavefunction dependent on the electric field strength:

$$|\psi''\rangle = |\psi'\rangle + e|\vec{E}| \sum \frac{\langle \phi_j | \hat{z} | \psi' \rangle}{E_{\psi'} - E_j} |\phi_j\rangle.$$

From here we can use the same procedures as in the zero-field case to obtain an expression for the hyperfine splittings dependent on the electric field strength. Using Ref. 2 as a guide, we expect modulation of the hyperfine splitting $\sim 0.1\%$ for electric fields $\sim 10^6 \frac{\text{V}}{\text{m}}$.

It may seem strange that the hyperfine Stark effect is a moot point in Tb³⁺, yet we expect to modulate the hyperfine structure constants by a non-negligible amount in TbPc₂. However, recall that the phthalocyanine molecules account for a large amount of electrostatic charge, in roughly planar distributions above and below the terbium ion. We expect that these large charge distributions are much more responsive to an electric field than the 4*f* orbitals in Tb³⁺. Therefore, with an electric field aligned along the z-axis, the easy axis of TbPc₂, the charge distribution of one of the ligands will want to be closer to the terbium ion while the charge distribution of the other will want to be further away. This breaks some of the symmetry of the molecule, and we expect that this would lead to a net interior dipole moment along the z-axis. Furthermore, the ligand field will be stronger near the terbium ion due to this emergent dipole moment, and so it will interact with the 4*f* orbitals more strongly than in the zero-field regime. We expect that this amplifies the hyperfine splitting by

a non-negligible amount. Conversely in Tb^{3+} , there is no ligand field and so the $4f$ electrons can only couple directly to the external electric field, which is an extremely weak effect as shown in section 3.6.

To enhance the hyperfine Stark effect, we want to think about ways to enhance the coupling of the ligand field to the $4f$ electrons of the terbium ion. One way to do this is to increase the strength of the emergent dipolar ligand field. Thinking in terms of multipole moments, we can increase the strength of a dipole moment by further breaking the symmetry of the molecule. For example, we could make the ligands distinguishable from each other by removing a single nitrogen atom or bonding chlorine atoms to the exterior hydrogens of just one of the ligands. This would create a small net dipole moment in the zero-field regime, which would become amplified in the presence of an external electric field. To make this even more drastic, we could replace one of the phthalocyanine molecules with a completely different planar ligand such as porphyrin, derivatives of hexagonal boron nitride, or perhaps a crown ether.

APPENDICES

A1 Wigner 3-j Symbols

The Wigner 3-j symbol is an alternative method for adding angular momenta to Clebsch-Gordan coefficients. It is also useful for simplifying integrals of three spherical harmonics.

A1.1 Symmetry Properties

A 3-j symbol is invariant under cyclic permutations of its columns:

$$\begin{pmatrix} j_1 & j_2 & j_3 \\ m_1 & m_2 & m_3 \end{pmatrix} = \begin{pmatrix} j_2 & j_3 & j_1 \\ m_2 & m_3 & m_1 \end{pmatrix} = \begin{pmatrix} j_3 & j_1 & j_2 \\ m_3 & m_1 & m_2 \end{pmatrix}$$

A 3-j symbol picks up a phase under interchange of its columns:

$$\begin{pmatrix} j_1 & j_2 & j_3 \\ m_1 & m_2 & m_3 \end{pmatrix} = (-1)^{j_1+j_2+j_3} \begin{pmatrix} j_2 & j_1 & j_3 \\ m_2 & m_1 & m_3 \end{pmatrix} = (-1)^{j_1+j_2+j_3} \begin{pmatrix} j_1 & j_3 & j_2 \\ m_1 & m_3 & m_2 \end{pmatrix}$$

Changing the sign of all m_i also causes a 3-j symbol to pick up a phase:

$$\begin{pmatrix} j_1 & j_2 & j_3 \\ -m_1 & -m_2 & -m_3 \end{pmatrix} = (-1)^{j_1+j_2+j_3} \begin{pmatrix} j_1 & j_2 & j_3 \\ m_1 & m_2 & m_3 \end{pmatrix}$$

A1.2 Selection rules

A 3-j symbol evaluates to 0 unless the following conditions are met:

$$m_1 + m_2 + m_3 = 0 \text{ and } |j_1 - j_2| \leq j_3 \leq j_1 + j_2$$

A1.3 Relation to Clebsch-Gordan Coefficients

Clebsch-Gordan coefficients can be expressed in terms of Wigner 3-j symbols as follows:

$$\langle j_1, m_1, j_2, m_2 | J, M_J \rangle = (-1)^{-j_1+j_2-M_J} \sqrt{2J+1} \begin{pmatrix} j_1 & j_2 & J \\ m_1 & m_2 & -M_J \end{pmatrix}$$

A1.4 Relation to Spherical Harmonics

We can also use the Wigner-3j symbols to simplify the integral of a product of three spherical harmonics:

$$\begin{aligned} & \int Y_{l_1 m_1}(\theta, \phi) Y_{l_2 m_2}(\theta, \phi) Y_{l_3 m_3}(\theta, \phi) \sin \theta d\theta d\phi \\ &= \sqrt{\frac{(2l_1+1)(2l_2+1)(2l_3+1)}{4\pi}} \begin{pmatrix} l_1 & l_2 & l_3 \\ 0 & 0 & 0 \end{pmatrix} \begin{pmatrix} l_1 & l_2 & l_3 \\ m_1 & m_2 & m_3 \end{pmatrix} \end{aligned}$$

A2 Gaunt Coefficients

Gaunt coefficients are very similar to products of Wigner 3-j symbols, especially in their relation to spherical harmonics.

A2.1 Relation to Spherical Harmonic and Wigner 3-j symbols

$$\begin{aligned} \text{Gaunt}(l_1, l_2, l_3, m_1, m_2, m_3) &= \int Y_{l_1 m_1}(\theta, \phi) Y_{l_2 m_2}(\theta, \phi) Y_{l_3 m_3}(\theta, \phi) \sin \theta d\theta d\phi \\ &= \sqrt{\frac{(2l_1+1)(2l_2+1)(2l_3+1)}{4\pi}} \begin{pmatrix} l_1 & l_2 & l_3 \\ 0 & 0 & 0 \end{pmatrix} \begin{pmatrix} l_1 & l_2 & l_3 \\ m_1 & m_2 & m_3 \end{pmatrix} \end{aligned}$$

REFERENCES

- [1] S. Thiele, F. Balestro, R. Ballou, S. Klyatskaya, M. Ruben, and W. Wernsdorfer, *Science* **344**, 1135 (2014), ISSN 0036-8075.
- [2] S. Thiele, *Read-out and coherent manipulation of an isolated nuclear spin using a single molecule magnet spin transistor*, Ph.D. thesis, Université de Grenoble (2014).
- [3] J. Townsend, *A Modern Approach to Quantum Mechanics*, International series in pure and applied physics (University Science Books, 2000), ISBN 9781891389139.
- [4] H. Hellwig, R. Vessot, M. Levine, P. Zitzewitz, D. Allan, and D. Glaze, *Instrumentation and Measurement*, *IEEE Transactions on* **19**, 200 (1970).
- [5] A. Dupays, A. Beswick, B. Lepetit, C. Rizzo, and D. Bakalov, *Physical Review A* **68** (2003).
- [6] J. Stark, *Nature* **92**, 401 (1913).
- [7] A. Dalgarno, J. T. Lewis, and D. R. Bates, *Proceedings of the Royal Society of London. Series A. Mathematical and Physical Sciences* **233**, 70 (1955).
- [8] E. Clementi, D. L. Raimondi, and W. P. Reinhardt, *The Journal of Chemical Physics* **47**, 1300 (1967).

- [9] J. M. Baker, J. R. Chadwick, G. Garton, and J. P. Hurrell, Proceedings of the Royal Society of London. Series A, Mathematical and Physical Sciences **286**, 352 (1965), ISSN 00804630.
- [10] N. Bohr, The London, Edinburgh, and Dublin Philosophical Magazine and Journal of Science **26**, 1 (1913).
- [11] M. L. Campbell, Journal of Chemical Education **75**, 1339 (1998).
- [12] I. I. Vrubel, A. A. Pervishko, H. Herper, B. Brena, O. Eriksson, and D. Yudin, Phys. Rev. B **101**, 125106 (2020).
- [13] A. Zangwill, *Modern electrodynamics* (Cambridge Univ. Press, Cambridge, 2013).